

# A geometric classification of traveling front propagation in the Nagumo equation with cut-off

N Popović

University of Edinburgh, School of Mathematics and Maxwell Institute for Mathematical Sciences, James Clerk Maxwell Building, King's Buildings, Mayfield Road, Edinburgh, EH9 3JZ, United Kingdom

E-mail: Nikola.Popovic@ed.ac.uk

**Abstract.** An important category of solutions to reaction-diffusion systems of partial differential equations is given by traveling fronts, which provide a monotonic connection between rest states and maintain a fixed profile when considered in a co-moving frame. Reaction-diffusion equations are frequently employed in the mean-field (continuum) approximation of discrete (many-particle) models; however, the quality of this approximation deteriorates when the number of particles is not sufficiently large. The (stochastic) effects of this discreteness have been modeled via the introduction of (deterministic) ‘cut-offs’ that effectively deactivate the reaction terms at points where the particle concentration is below a certain threshold. In this article, we present an overview of the effects of such a cut-off on the front propagation dynamics in a prototypical reaction-diffusion system, the classical Nagumo equation. Our analysis is based on the method of geometric desingularization (‘blow-up’), in combination with dynamical systems techniques such as invariant manifolds and normal forms. Using these techniques, we categorize front propagation in the cut-off Nagumo equation in dependence of a control parameter, and we classify the corresponding propagation regimes (‘pulled,’ ‘pushed,’ and ‘bistable’) in terms of the bifurcation structure of a projectivized system of equations that is obtained from the original traveling front problem, after blow-up. In particular, our approach allows us to determine rigorously the asymptotics (in the cut-off parameter) of the correction to the front propagation speed in the Nagumo equation that is due to a cut-off. Moreover, it explains the structure of that asymptotics (logarithmic, superlinear, or sublinear) in dependence of the front propagation regime. Finally, it enables us to calculate the corresponding leading-order coefficients in the resulting expansions in closed form.

## 1. Introduction

Front propagation in reaction-diffusion systems represents a fundamental topic in non-equilibrium physics. Traveling fronts are monotonic connections between rest states that retain a fixed profile in an appropriately defined (‘co-moving’) frame; they are frequently relevant in the asymptotic (long-time) limit of such systems. For the sake of definiteness, we will only consider front propagation in the family of scalar reaction-diffusion equations that is given by

$$\frac{\partial\phi}{\partial t} = \frac{\partial^2\phi}{\partial x^2} + f(\phi), \quad (1)$$

where  $(t, x) \in \mathbb{R}^+ \times \mathbb{R}$ ,  $\phi(t, x) \in \mathbb{R}$ , and  $f$  denotes a smooth function with  $f(\phi^-) = 0 = f(\phi^+)$ ; without loss of generality, we assume that the two rest states at  $\phi^-$  and  $\phi^+$  have been rescaled

to 1 and 0, respectively. Equation (1) has found widespread use throughout the sciences, and has *e.g.* been applied in population dynamics, genetics, thermal combustion, mathematical neuroscience, chemical kinetics, and fluid dynamics; see *e.g.* [1, 2] for details and references.

As is well-known [3, 4], front solutions propagating between the rest states at 1 and 0 in (1) can be classified in terms of the reaction function  $f$ , which is said to be of type I if it is strictly positive on  $(0, 1)$ , while it is of type II if it changes sign on that interval exactly once. Generically, one assumes that  $f$  is negative on some subinterval  $(0, \alpha)$  of  $(0, 1)$ , with  $\alpha \in (0, 1)$ , whereas it is positive on  $(\alpha, 1)$ ; moreover, one requires  $\int_0^1 f(\phi) d\phi > 0$  for the front propagation speed  $c$  to be positive [2], as specified in detail below.

For type I-functions with  $f'(0) > 0$ , zero is an unstable rest state of (1); the corresponding front solution can be either ‘pulled’ or ‘pushed.’ Pulled fronts propagate at the linear spreading speed  $c^* = 2\sqrt{f'(0)}$  of perturbations about the zero rest state in (1). (Intuitively speaking, the front is ‘pulled’ along by the linearization of  $f$  about zero.) A prototypical example is provided by the Fisher-Kolmogorov-Petrovskii-Piscounov (FKPP) equation [5], which is obtained for  $f(\phi) = \phi(1 - \phi)$  in (1). By contrast, the propagation speed of pushed fronts, termed  $c^\dagger$ , is higher than  $c^*$ , as is for example the case in the classical Nagumo equation [1, 2], which is defined by

$$\frac{\partial \phi}{\partial t} = \frac{\partial^2 \phi}{\partial x^2} + \phi(1 - \phi)(\phi - \gamma), \quad (2)$$

with  $\gamma$  a real parameter: for  $\gamma \in (-\frac{1}{2}, 0)$ , Equation (2) supports front solutions with  $c^\dagger = \frac{1}{\sqrt{2}} - \sqrt{2}\gamma$ , while the propagation speed obtained from linearization about zero is given by  $c^* = 2\sqrt{-\gamma}$ . (The nonlinear dynamics behind the front drives, or ‘pushes,’ front propagation in this regime.)

**Remark 1.** In both regimes, traveling fronts exist for a continuum of speeds, with  $c \geq c^*$ ; fronts propagating at different speeds are distinguished by their decay properties at 0 [6, 7]. However, for sufficiently localized initial conditions, one particular front is ‘selected’ by the system: in the pulled regime, that front propagates at the linear spreading speed  $c^*$ , while the propagation speed  $c^\dagger$  in the pushed regime is higher, as stated above.  $\square$

For type-II reaction functions with  $f'(0) < 0$ , zero is a (meta)stable rest state of (1). If, additionally,  $f(\alpha) = 0$  for some  $\alpha \in (0, 1)$ , the front is called ‘bistable’ and propagates at a speed  $c$  that is not obviously related to the linearization of  $f$  at 0; a prototypical example is again given by the Nagumo equation, with  $\gamma \in (0, \frac{1}{2})$  in (2). Moreover, the front propagation speed is unique, *i.e.*, there exists exactly one traveling front solution in that regime.

The reader is referred to the reviews in [8] and [9] for an exhaustive discussion of this classification, and of the physical implications thereof.

**Remark 2.** If  $f'(0) = 0$ , the rest state at 0 is neutrally stable, and a transition occurs between the generic types I and II, as is the case in the family of scalar equations with degenerate polynomial potential  $f(\phi) = \phi^m(1 - \phi)$  in (1), for  $m \geq 2$ ; that family, which includes the Zeldovich equation ( $m = 2$ ), was analyzed in [4] and [10], as well as rigorously in [7] and [11].  $\square$

Reaction-diffusion equations of the form in (1) are often employed in the large-scale (continuum) approximation of discrete,  $N$ -particle systems [12, 13]. The quality of this approximation, while oftentimes surprisingly good, deteriorates as the number of particles  $N$  decreases, since stochastic fluctuations need to be taken into account at a microscopic scale. (In particular, the front propagation speed is frequently misestimated, even when the qualitative front profile is accurately reproduced.)

Recently [5, 14], it has been suggested to model the stochastic effects of this discreteness by

introducing a deterministic ‘cut-off’ at the zero rest state in (1):

$$\frac{\partial \phi}{\partial t} = \frac{\partial^2 \phi}{\partial x^2} + f(\phi)\theta(\phi, \varepsilon). \quad (3)$$

Simply speaking, the cut-off function  $\theta$  dampens the reaction amplitude whenever the particle concentration  $\phi$  in (3) lies below a certain threshold. In  $N$ -particle systems, no particles are available to react when  $\phi$  is below the threshold  $N^{-1}$ ; correspondingly, the reaction terms in (1) are ‘cut-off’ in an  $N^{-1}$ -neighborhood of 0. In the simplest case, where  $\theta$  is the Heaviside cut-off  $H$ , with

$$H(\phi - \varepsilon) \equiv 0 \quad \text{for} \quad \phi < \varepsilon \quad \text{and} \quad H(\phi - \varepsilon) \equiv 1 \quad \text{for} \quad \phi \geq \varepsilon, \quad (4)$$

the function  $f$  is simply set to zero for  $\phi < \varepsilon \equiv N^{-1}$ .

A cut-off substantially changes the characteristics of the front propagation dynamics of the family of reaction-diffusion equations in (1): in [5], Brunet and Derrida studied traveling fronts in the cut-off FKPP equation, with  $f(\phi) = \phi(1 - \phi)$  in (3). They found that the correction  $\Delta c$  to the linear spreading speed  $c^* = 2$  that is induced by a Heaviside cut-off is given by  $\Delta c = -\pi^2(\ln \varepsilon)^{-2}[1 + o(1)]$ , for  $\varepsilon$  sufficiently small; moreover, they conjectured that this leading-order asymptotics is universal over a wide range of cut-off functions  $\theta$ . Finally, they argued that a Heaviside cut-off always selects a unique front solution for (3), even when the corresponding equation without cut-off supports an entire family of solutions. (A comprehensive review of the physical aspects of Brunet and Derrida’s conjecture can *e.g.* be found in [8].)

Starting with [5], a growing body of work has emerged on the front propagation dynamics of cut-off reaction-diffusion systems and, in particular, on the change in front propagation speed that is caused by a cut-off. Thus, it has been shown that the effects of a cut-off depend strongly on the type of reaction function  $f$  in (3): specifically, cut-offs reduce the propagation speed of pulled fronts, whereas they speed up pushed and bistable fronts [10]. Similarly, the correction  $\Delta c$  to the propagation speed that is due to a cut-off is logarithmic in  $\varepsilon$  in the pulled propagation regime, which implies that the front speed converges slowly to its continuum value  $c^*$  as  $\varepsilon \rightarrow 0$  [3, 6]. By contrast,  $\Delta c$  is sublinear and superlinear in  $\varepsilon$  in the pushed and bistable regimes, respectively; correspondingly, the convergence to the continuum speed is fast in those regimes [10, 15, 16, 17].

Recently, these results have been made rigorous by us, using the method of geometric desingularization (‘blow-up’) [18, 19]. Front propagation in the cut-off FKPP equation, as well as in certain generalizations thereof, was studied geometrically in [6]; in particular, we confirmed the leading-order expansion for  $\Delta c$ , as stipulated by Brunet and Derrida [5], and we gave a proof of their conjecture for a very general family of cut-off functions  $\theta$ . In the follow-up article [15], we investigated the effects of a cut-off on bistable traveling fronts, and we obtained corresponding results for the asymptotics of  $\Delta c$ : we proved that  $\Delta c$  is positive, and we explained the occurrence of fractional powers of  $\varepsilon$  in the resulting expansion. Analogous results on the effects of a cut-off on the front propagation dynamics in the pushed regime will be given in the upcoming article [16].

In the present article, we provide a systematic overview of front propagation in the Nagumo equation, as given in (2), in the presence of a cut-off. In particular, we classify the resulting front solutions geometrically, in terms of the dynamics of a rescaled (‘projectivized’) version of (2) in the various propagation regimes, *i.e.*, in dependence of the parameter  $\gamma$ . Without loss of generality, we will only consider the case where  $\theta$  is the Heaviside cut-off  $H$  defined in (4) here:

$$\frac{\partial \phi}{\partial t} = \frac{\partial^2 \phi}{\partial x^2} + \phi(1 - \phi)(\phi - \gamma)H(\phi - \varepsilon). \quad (5)$$

(Other choices of cut-off functions can be studied in a similar fashion; see [6, 15, 20, 21] for details.) As is well-known, Equation (2) (without cut-off) supports traveling front solutions that propagate between  $(\phi^- =)1$  and  $(\phi^+ =)0$  for an entire (real) interval of  $\gamma$ -values. (The third rest state of (2), which is located at  $\phi^o = \gamma$ , is of no interest to us here.) The stability of these rest states is determined by the value of the parameter  $\gamma$  [22]: specifically, the rest states at 1 and  $\gamma$  are stable, while the rest state at 0 is unstable for  $\gamma \in [-1, 0)$  in (2); conversely, for  $\gamma \in [0, 1)$ , the rest states at 1 and 0 are stable, while the rest state at  $\gamma$  is unstable.

Traveling front solutions to (2) are conveniently analyzed in the co-moving frame that is defined by the traveling wave variable  $\xi = x - ct$ . Writing  $u(\xi) = \phi(t, x)$  for the corresponding front, we obtain the traveling front equation

$$u'' + cu' + u(1 - u)(u - \gamma)H(u - \varepsilon) = 0, \quad (6)$$

where  $c$  denotes the front propagation speed. Since we are interested in front solutions that propagate with non-zero speed from 1 into 0, we will restrict ourselves to  $\gamma \in [-1, \frac{1}{2})$  in (6): multiplying the traveling front equation

$$u'' + cu' + u(1 - u)(u - \gamma) = 0 \quad (7)$$

that corresponds to Equation (2) with  $u'$ , integrating the result over  $\xi$ , and taking into account that  $u' \rightarrow 0$  as  $\xi \rightarrow \pm\infty$ , one finds

$$c \int_{-\infty}^{\infty} [u'(\xi)]^2 d\xi = \int_0^1 u(1 - u)(u - \gamma) du = \frac{1}{12}(1 - 2\gamma).$$

Hence, the front propagation speed  $c$  that is realized in the absence of a cut-off must change sign (and, indeed, become negative) when  $\gamma > \frac{1}{2}$ . In particular,  $c$  vanishes for  $\gamma = \frac{1}{2}$ ; thus,  $\xi = x$ , and the corresponding solution to (7) becomes stationary. (A detailed analysis of the effects of a linear cut-off in (2) in that case can be found in [21].) Beyond this so-called ‘Maxwell point,’ *i.e.*, for  $\gamma \in (\frac{1}{2}, 1)$ , the traveling front reverses direction. Correspondingly, the rest state at 1 becomes ‘dominant’ [2] and loses stability, as observed also independently in [23].

This article is organized as follows. In Section 2, we revisit the geometric framework that was first introduced in [6], and we adapt that framework for our study of front propagation in the cut-off Nagumo equation; see also [15, 16, 20, 21]. Then, in Section 3, we discuss the propagation regimes that can be realized in Equation (5). For the sake of completeness, we first review the bistable and pushed regimes that were analyzed in detail in [15] and [16], respectively, and we summarize the main results obtained there. Then, we show how the pulled propagation regime can be studied in the context of theory previously developed in [6]. Specifically, we introduce a coordinate transformation that reduces Equation (5) to an FKPP-like equation with cut-off. We deduce the existence of traveling fronts in the presence of a cut-off in the resulting, transformed equation, and we infer the leading-order  $\varepsilon$ -asymptotics of the propagation speed  $c$  of these fronts. Reverting to the original coordinates, we obtain corresponding results for Equation (5). Then, we discuss three boundary cases that limit the pulled, pushed, and bistable regimes. Finally, we combine these findings and interpret them, completing our classification of front propagation in the cut-off Nagumo equation. In Section 4, we summarize our results, and we discuss possible topics for future research.

## 2. Geometric framework

In this section, we review the geometric framework on which our classification of the front propagation dynamics of Equation (5) is based. In particular, we outline the construction of a singular heteroclinic connection in the corresponding traveling front equation (6); details can be found in [6], where that same framework was first introduced for the study of the FKPP equation with cut-off, as well as in [15, 16, 20, 21].

## 2.1. Background

As indicated in the Introduction, our classification of front propagation in the cut-off Nagumo equation draws on geometric methods from dynamical systems theory and, in particular, on the so-called blow-up technique (geometric desingularization) [18, 19]. Blow-up complements the geometric singular perturbation theory initiated by Fenichel [24]; it is essentially a sophisticated coordinate transformation that regularizes the dynamics in neighborhoods of singularities, allowing one to apply standard dynamical systems techniques. Moreover, it identifies the relevant asymptotics near these singularities and, in particular, the nature of the dependence of that asymptotics on the corresponding perturbation parameter.

Beginning with [7], we have shown that the blow-up technique is ideally suited to the study of front propagation in degenerate reaction-diffusion systems, *i.e.*, in equations in which the reaction terms exhibit non-hyperbolic behavior (at 0), as is the case for  $f(\phi) = \phi^m(1 - \phi)$  ( $m \geq 2$ ) in (1) [20], or, alternatively, in cut-off equations of the type in (3), where the degeneracy is caused by a cut-off at the zero rest state: in addition to introducing a non-hyperbolicity (in the form of zero eigenvalues) in the traveling front equation (6), the cut-off also renders the corresponding vector field discontinuous at  $u = \varepsilon$ .

As in [6, 15, 16, 20, 21], our study of front propagation in (5) is based on a geometric (phase space) analysis of the extended, equivalent first-order system that is obtained from (6) by introducing the new variable  $v = u'$  and by appending the trivial  $\varepsilon$ -dynamics:

$$u' = v, \tag{8a}$$

$$v' = -cv - u(1 - u)(u - \gamma)H(u - \varepsilon), \tag{8b}$$

$$\varepsilon' = 0. \tag{8c}$$

Fronts that propagate between the rest states at 1 and 0 in (5) correspond to heteroclinic connections between the equilibrium points  $Q_\varepsilon^+ := (0, 0, \varepsilon)$  and  $Q_\varepsilon^- := (1, 0, \varepsilon)$  of (8), for  $\varepsilon$  sufficiently small. (The third equilibrium point, which is located at  $Q_\varepsilon^o := (\gamma, 0, \varepsilon)$ , is the equivalent of the rest state at  $\gamma$  in (5), and is of no interest to us here.) For future reference, we note that, in the singular limit as  $\varepsilon \rightarrow 0^+$ , these equilibria reduce to  $Q_0^- = (1, 0, 0)$  and  $Q_0^+ = (0, 0, 0)$ , which are equilibrium points for the first-order system that is obtained from (7), in the absence of a cut-off:

$$u' = v, \tag{9a}$$

$$v' = -cv - u(1 - u)(u - \gamma). \tag{9b}$$

Correspondingly, the value of the front propagation speed  $c$  for which a heteroclinic connection is realized in (9) is given by  $c_0$ . (Here, we note that  $c_0$  can equal either  $c^*(= 2\sqrt{-\gamma})$  or  $c^\dagger(= \frac{1}{\sqrt{2}} - \sqrt{2}\gamma)$ , depending on the front propagation regime under consideration; see Sections 3.1 through 3.4 below for details.) The properties of  $Q_0^-$  and  $Q_0^+$  in dependence of  $\gamma \in [-1, \frac{1}{2})$  and  $c_0$ , in the context of the first-order system (9), as well as the eigenvalues  $\lambda_\mp^- = -\frac{c_0}{2} \mp \sqrt{\frac{c_0^2}{4} + 1 - \gamma}$  and  $\lambda_\mp^+ = -\frac{c_0}{2} \mp \sqrt{\frac{c_0^2}{4} + \gamma}$  of the associated linearization about these points, are summarized in Tables 1 and 2, respectively. (In particular, we remark that the stability of  $Q_0^\mp$  is the converse of that of the corresponding rest states at  $\phi^\mp$  of the partial differential equation (2).)

The degeneracy that is introduced by the cut-off into (8) can be removed by ‘blowing up’ the origin  $Q_0^+$  to an invariant two-sphere in three-space; the dynamics on that sphere is conveniently studied by introducing (local) coordinates, which are essentially rescalings of the state variables  $u$  and  $v$  and the parameter  $\varepsilon$ . Two such coordinate systems (‘charts’) are required here: a ‘family chart,’ which corresponds to an  $\varepsilon$ -rescaling that is uniformly valid in any bounded neighborhood of the north pole of the sphere, and a ‘phase-directional chart,’ which projectivizes the dynamics

**Table 1.** The equilibrium point  $Q_0^-$  in dependence of  $\gamma$  and  $c_0$ .

| $\gamma$             | $\lambda_{\mp}^-$                         | type   | stability |
|----------------------|---|--------|-----------|
| -1                   | $-1 \mp \sqrt{3}$                         | saddle | unstable  |
| $(-1, -\frac{1}{2})$ | $-\sqrt{-\gamma} \mp \sqrt{1-2\gamma}$    | saddle | unstable  |
| $-\frac{1}{2}$       | $-\frac{3}{\sqrt{2}}, \frac{1}{\sqrt{2}}$ | saddle | unstable  |
| $(-\frac{1}{2}, 0)$  | $(\gamma-1)\sqrt{2}, \frac{1}{\sqrt{2}}$  | saddle | unstable  |
| 0                    | $-\sqrt{2}, \frac{1}{\sqrt{2}}$           | saddle | unstable  |
| $(0, \frac{1}{2})$   | $(\gamma-1)\sqrt{2}, \frac{1}{\sqrt{2}}$  | saddle | unstable  |

**Table 2.** The equilibrium point  $Q_0^+$  in dependence of  $\gamma$  and  $c_0$ .

| $\gamma$             | $\lambda_{\mp}^+$                     | type            | stability |
|----------------------|---------------------------------------|-----------------|-----------|
| -1                   | -1 (double)                           | degenerate node | stable    |
| $(-1, -\frac{1}{2})$ | $-\sqrt{-\gamma}$ (double)            | degenerate node | stable    |
| $-\frac{1}{2}$       | $-\frac{1}{\sqrt{2}}$ (double)        | degenerate node | stable    |
| $(-\frac{1}{2}, 0)$  | $-\frac{1}{\sqrt{2}}, \sqrt{2}\gamma$ | node            | stable    |
| 0                    | $-\frac{1}{\sqrt{2}}, 0$              | saddle-node     | stable    |
| $(0, \frac{1}{2})$   | $-\frac{1}{\sqrt{2}}, \sqrt{2}\gamma$ | saddle          | unstable  |

near the equator. The corresponding rescaled coordinates will be denoted by  $(U, V, \varepsilon)$  and  $(u, W, E)$ , respectively.

The phase-space of the cut-off first order system (8) naturally decomposes into three regions, an outer region (where  $u > \varepsilon$  and the flow is unaffected by the cut-off), an inner region (where  $u < \varepsilon$  and the vector field is cut-off), and an intermediate region, with  $u = O(\varepsilon)$ , that represents the boundary between the two. The flow of (8) in the inner and intermediate regions (after blow-up) will be analyzed separately in the family and phase-directional charts, respectively, while the dynamics in the outer region is described in the original  $(u, v, \varepsilon)$ -variables. In particular, blow-up resolves the singular nature of the transition between the inner and outer regions; specifically, it regularizes the singular limit as  $\varepsilon \rightarrow 0^+$  in the intermediate region, allowing for the construction of a singular heteroclinic connection  $\Gamma$  between the relevant equilibria  $Q_0^-$  and  $Q_0^+$  of (8). Then, invariant manifold theory can be applied to show that this connection will persist, for  $\varepsilon$  sufficiently small, in the intersection of the unstable manifold  $\mathcal{W}^u(Q_\varepsilon^-)$  of  $Q_\varepsilon^-$  with the stable manifold  $\mathcal{W}^s(Q_\varepsilon^+)$  of  $Q_\varepsilon^+$ . The resulting persistent heteroclinic corresponds to a traveling front solution for the cut-off Nagumo equation (5); moreover, the corresponding persistence proof determines the  $\varepsilon$ -asymptotics of the propagation speed  $c$  of that front, as discussed in detail in Section 3 below.

**Remark 3.** The blow-up transformation introduced above, in an informal fashion, can more formally be written as a mapping of the form

$$\varphi : \begin{cases} \mathbb{S}^2 \times [0, r_0] \rightarrow \mathbb{R}^3, \\ (\bar{u}, \bar{v}, \bar{\varepsilon}, \bar{r}) \mapsto (\bar{r}\bar{u}, \bar{r}\bar{v}, \bar{r}\bar{\varepsilon}), \end{cases}$$

where  $\mathbb{S}^2$  denotes the 2-sphere in  $\mathbb{R}^3$ , while  $r_0$  is a positive constant. In particular, the inverse mapping  $\varphi^{-1}$  maps the origin  $Q_0^+$  to  $\mathbb{S}^2$ , as required; cf. [6], where this transformation was employed in the analysis of the FKPP equation with cut-off. It was subsequently applied in [25] as well as in [15, 16, 20, 21]; for reference, we remark that the phase-directional and family charts defined above were labeled  $K_1$  and  $K_2$  there, respectively. To keep our presentation accessible, we will not pursue that more formal approach here; a detailed, rigorous introduction to the blow-up technique can *e.g.* be found in [18].  $\square$

## 2.2. Outer region

The flow in the outer region, where  $u > \varepsilon$ , is governed by the first-order system (9) that is obtained from Equation (7) (without cut-off), as  $H \equiv 1$  there; recall the definition of  $H$  in (4). The traveling front solution that propagates between the rest states at 1 and 0 in (2), with propagation speed  $c_0$ , corresponds to a heteroclinic connection  $\Gamma$  between the two equilibrium points  $Q_0^- = (1, 0, 0)$  and  $Q_0^+ = (0, 0, 0)$  which is realized for  $c = c_0$  in (9), as discussed above. Moreover, that connection coincides with the unstable manifold  $\mathcal{W}^u(Q_0^-)$  of  $Q_0^-$ . In general, for  $\varepsilon \in (0, \varepsilon_0]$ , with  $\varepsilon_0$  positive and sufficiently small, the unstable manifold  $\mathcal{W}^u(Q_\varepsilon^-)$  of  $Q_\varepsilon^-$  is analytic in the state variables  $u$  and  $v$  and in the parameter  $c$ . Hence, writing  $c = c_0 + (c - c_0) = c_0 + \Delta c$ , with  $\Delta c = o(1)$ , we may assume an expansion of the form

$$v(u, c) = \sum_{j=0}^{\infty} \frac{1}{j!} \frac{\partial^j v}{\partial c^j}(u, c_0) (\Delta c)^j \quad (10)$$

for that manifold.

**Remark 4.** The expansion in (10) is only implicitly  $\varepsilon$ -dependent, as it follows from (9) that any such dependence must enter through  $c$ . Correspondingly, in the extended system (8), the unstable manifold  $\mathcal{W}^u(\ell^-)$  of the line of equilibria  $\ell^- = \{(1, 0, \varepsilon) \mid \varepsilon \in [0, \varepsilon_0]\}$  is a trivial foliation in  $\varepsilon$ , with fibers  $\mathcal{W}^u(Q_\varepsilon^-)$ .  $\square$

As shown in [15, 20], only the first two terms in (10) play a role to the order considered here: the leading-order term  $v(u, c_0)$  again corresponds to  $\mathcal{W}^u(Q_0^-)$  or, equivalently, to the orbit  $\Gamma$ , while the next-order (linear) term in  $\Delta c$  is found as the solution  $\frac{\partial v}{\partial c}(u, c_0)$  of the variational equation that is associated with (9), taken along  $v(u, c_0)$ . That equation is obtained as follows: we first rewrite (9) with  $u$  as the independent variable, *i.e.*, we divide (9b) (formally) by (9a):

$$v \frac{dv}{du} = -cv - u(1-u)(u-\gamma). \quad (11)$$

Then, we differentiate (11) with respect to  $c$  and substitute  $c_0$  and  $v(u, c_0)$ , as well as (11), into the resulting equation to find

$$\frac{\partial}{\partial u} \left( \frac{\partial v}{\partial c}(u, c_0) \right) = -1 + \frac{u(1-u)(u-\gamma)}{[v(u, c_0)]^2} \frac{\partial v}{\partial c}(u, c_0). \quad (12)$$

For the variational equation (12) to have a closed-form solution, it is necessary that  $c_0$  and  $v(u, c_0)$  are known explicitly, as discussed in detail in [15] and [20]. In particular, Equation (12) can be solved exactly in the bistable and pushed propagation regimes; the relevant results from [15] and [16] will be recalled in Sections 3.1 and 3.2 below; cf. also [20, 21]. (Since no closed-form solution to the traveling front equation (7) seems to be known in the pulled propagation regime [6], it follows that (12) can have no exact solution in that case, either.)

Next, we introduce a section for the flow of (8), as follows: for  $\rho \geq \varepsilon_0$  and  $v_0 > c_0$  positive and fixed, we write  $\Sigma^-$  for the hyperplane

$$\Sigma^- = \{(\rho, v, \varepsilon) \mid (v, \varepsilon) \in [-v_0, 0] \times [0, \varepsilon_0]\} \quad (13)$$

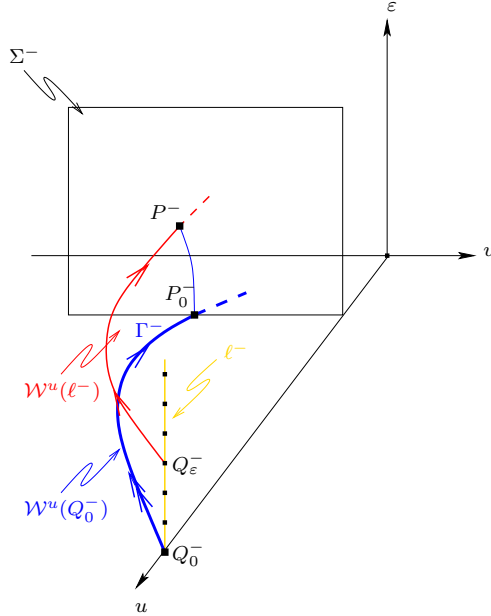


**Figure 1.** The geometry in the outer region.

in  $(u, v, \varepsilon)$ -space, and we denote the point of intersection of  $\Gamma$  with  $\Sigma^-$  by  $P_0^- = (\rho, v_0^-, 0)$ , where  $v_0^- = v(\rho, c_0)$ . Similarly, we write  $P^-$  for the point of intersection of  $\mathcal{W}^u(Q_\varepsilon^-)$  with  $\Sigma^-$ ; in particular, we suppress the dependence of that point on the parameters  $c$  and  $\varepsilon$ , for brevity. Finally, the segment of the singular heteroclinic connection  $\Gamma$  that is located in this outer region, *i.e.*, in  $\{u \geq \rho\}$ , will be labeled  $\Gamma^-$ ; the resulting geometry is summarized in Figure 1.

### 2.3. Inner region

In the inner region, with  $u < \varepsilon$ , the dynamics of Equation (5) is cut-off, as the Heaviside cut-off  $H$  vanishes there; see again (4). The flow in this region is desingularized via the family rescaling

$$u = \varepsilon U, \quad v = \varepsilon V, \quad \text{and} \quad \varepsilon = \varepsilon; \quad (14)$$

the governing equations that are obtained from (8), in the rescaled  $(U, V, \varepsilon)$ -coordinates, read

$$U' = V, \quad (15a)$$

$$V' = -cV, \quad (15b)$$

$$\varepsilon' = 0. \quad (15c)$$

Although for  $\varepsilon$  fixed, all points on the  $U$ -axis are equilibria of (15), we only consider points on the line  $\ell^+ = \{(0, 0, \varepsilon) \mid \varepsilon \in [0, \varepsilon_0]\}$  here, as only the latter can correspond to  $Q_\varepsilon^+$  in the original  $(u, v, \varepsilon)$ -variables.

In the singular limit as  $\varepsilon \rightarrow 0^+$  in (8), the front propagation speed  $c$  reduces to  $c_0$ ; cf. Section 2.1. The unique solution of the resulting singular equation in this inner region, *i.e.*, of

$$\frac{dV}{dU} = -c_0, \quad \text{with} \quad V(0) = 0, \quad (16)$$

is given by  $V(U) = -c_0 U$ ; the orbit corresponding to that solution, which we denote by  $\Gamma^+$ , yields precisely the stable manifold  $\mathcal{W}^s(Q_0^+)$  of the origin  $Q_0^+$  in the family chart.

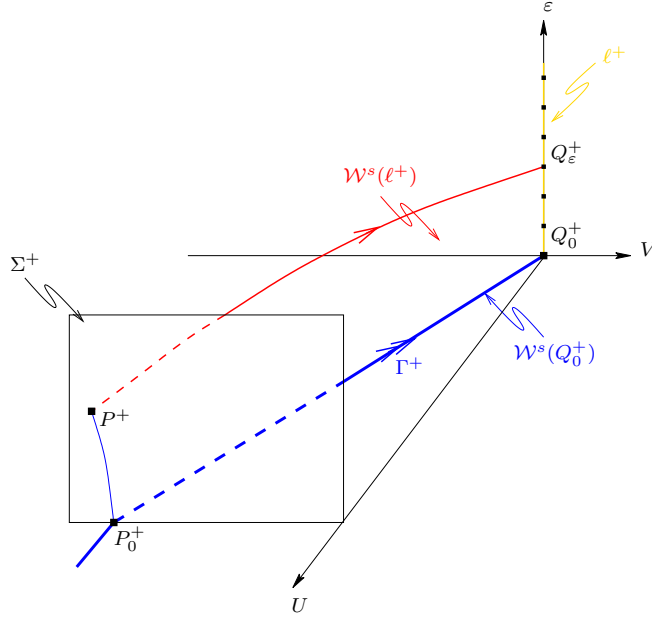


**Figure 2.** The geometry in the inner region.

Next, we define the section  $\Sigma^+$  for the flow of (15) via

$$\Sigma^+ = \{(1, V, \varepsilon) \mid (V, \varepsilon) \in [-v_0, 0] \times [0, \varepsilon_0]\}, \quad (17)$$

with  $v_0 > 0$  as in (13). Since  $u < \varepsilon$  is equivalent to  $U < 1$ , by (14),  $\Sigma^+$  naturally separates the inner region, where the dynamics of (8) is governed by the simplified (cut-off) equations in (15), from the outer region, where that dynamics is unaffected by the cut-off, and is described by (9). Correspondingly,  $\Gamma^+$  gives the portion of the singular orbit  $\Gamma$  that is located in  $\{U < 1\}$ . The point of intersection of  $\Gamma^+$  with  $\Sigma^+$  will be labeled  $P_0^+ = (1, v_0^+, 0)$ ; in particular, we note that  $v_0^+ = -c_0$ . Finally, we write  $P^+$  for the point of intersection of  $\mathcal{W}^s(Q_\varepsilon^+)$  with  $\Sigma^+$ ; see Figure 2 for a summary of the geometry in this inner region.

#### 2.4. Intermediate region

The dynamics in the intermediate region, where  $u = O(\varepsilon)$ , is again governed by the first-order system (9) (without cut-off), since  $H \equiv 1$  there; recall Section 2.2. Hence, in the corresponding phase-directional coordinates

$$u = u, \quad v = uW, \quad \text{and} \quad \varepsilon = uE, \quad (18)$$

the governing equations are given by

$$u' = uW, \quad (19a)$$

$$W' = -cW - W^2 - (1 - u)(u - \gamma), \quad (19b)$$

$$E' = -EW. \quad (19c)$$

Since  $c$  evaluates to  $c_0$  in the singular limit as  $\varepsilon \rightarrow 0^+$  in (9), we find that the two principal equilibria of (19) in this intermediate region are located at  $P_- = (0, \lambda_-^+, 0)$  and  $P_+ = (0, \lambda_+^+, 0)$ , where  $\lambda_\mp^+ = -\frac{c_0}{2} \mp \sqrt{\frac{c_0^2}{4} + \gamma}$ , as defined in Section 2.2. Since, moreover, the rescaling in (18)

**Table 3.** The equilibrium point  $P_-$  in dependence of  $\gamma$  and  $c_0$ .

| $\gamma$             | $P_-$                         | $\lambda_-^+, -c_0 - 2\lambda_-^+, -\lambda_-^+$                           | type        |
|----------------------|-------------------------------|--|-------------|
| -1                   | $(0, -1, 0)$                  | -1, 0, 1   | saddle-node |
| $(-1, -\frac{1}{2})$ | $(0, -\sqrt{-\gamma}, 0)$     | $-\sqrt{-\gamma}, 0, \sqrt{-\gamma}$                                       | saddle-node |
| $-\frac{1}{2}$       | $(0, -\frac{1}{\sqrt{2}}, 0)$ | $-\frac{1}{\sqrt{2}}, 0, \frac{1}{\sqrt{2}}$                               | saddle-node |
| $(-\frac{1}{2}, 0)$  | $(0, -\frac{1}{\sqrt{2}}, 0)$ | $-\frac{1}{\sqrt{2}}, \frac{1}{\sqrt{2}}(1 + 2\gamma), \frac{1}{\sqrt{2}}$ | saddle      |
| 0                    | $(0, -\frac{1}{\sqrt{2}}, 0)$ | $-\frac{1}{\sqrt{2}}, \frac{1}{\sqrt{2}}, \frac{1}{\sqrt{2}}$              | saddle      |
| $(0, \frac{1}{2})$   | $(0, -\frac{1}{\sqrt{2}}, 0)$ | $-\frac{1}{\sqrt{2}}, \frac{1}{\sqrt{2}}(1 + 2\gamma), \frac{1}{\sqrt{2}}$ | saddle      |

**Table 4.** The equilibrium point  $P_+$  in dependence of  $\gamma$  and  $c_0$ .

| $\gamma$             | $P_+$                         | $\lambda_+^+, -c_0 - 2\lambda_+^+, -\lambda_+^+$                    | type        |
|----------------------|-------------------------------|---|-------------|
| -1                   | $(0, -1, 0)$                  | -1, 0, 1  | saddle-node |
| $(-1, -\frac{1}{2})$ | $(0, -\sqrt{-\gamma}, 0)$     | $-\sqrt{-\gamma}, 0, \sqrt{-\gamma}$                                | saddle-node |
| $-\frac{1}{2}$       | $(0, -\frac{1}{\sqrt{2}}, 0)$ | $-\frac{1}{\sqrt{2}}, 0, \frac{1}{\sqrt{2}}$                        | saddle-node |
| $(-\frac{1}{2}, 0)$  | $(0, \sqrt{2}\gamma, 0)$      | $\sqrt{2}\gamma, -\frac{1}{\sqrt{2}}(1 + 2\gamma), -\sqrt{2}\gamma$ | saddle      |
| 0                    | $(0, 0, 0)$                   | $0, -\frac{1}{\sqrt{2}}, 0$   | saddle-node |
| $(0, \frac{1}{2})$   | $(0, \sqrt{2}\gamma, 0)$      | $\sqrt{2}\gamma, -\frac{1}{\sqrt{2}}(1 + 2\gamma), -\sqrt{2}\gamma$ | saddle      |

projectivizes the flow of (9) in a small- $u$  neighborhood of  $Q_\varepsilon^+$ , as  $W = \frac{v}{u} = \frac{u'}{u}$ , the points  $P_\mp$  correspond to the two eigendirections of the linearization about  $Q_0^+$ ; recall Table 2, where the stability of  $Q_0^+$  is characterized in dependence of  $\gamma \in [-1, \frac{1}{2}]$ .

**Remark 5.** Other equilibrium points for (19) are found at  $(\gamma, 0, E)$  and  $(1, 0, E)$ ; however, these points, which correspond to the original equilibria  $Q_\varepsilon^o$  and  $Q_\varepsilon^-$  of (9), respectively, after transformation to phase-directional coordinates, are of no interest to us in this intermediate region.  $\square$

Linearizing (19) about the two points  $P_\mp$ , we find the eigenvalues  $\lambda_\mp^+, -c_0 - 2\lambda_\mp^+$ , and  $-\lambda_\mp^+$ , respectively. Consequently, the character of these equilibria again depends substantially on the front propagation regime under consideration, in accordance with the change in stability of  $Q_0^+$  as  $\gamma$  is varied in  $[-1, \frac{1}{2}]$ ; see Tables 3 and 4 for a summary of the stability properties of  $P_-$  and  $P_+$ , respectively, in dependence of  $\gamma$  and  $c_0$ . The corresponding dynamics in the intermediate region is illustrated in Figure 3; in particular, the geometry of the resulting local flow about  $P_-$  and  $P_+$  is determined by the ratios of the eigenvalues  $\lambda_\mp^-$  and  $\lambda_\mp^+$ , respectively. As will become clear in the following, the relevant equilibrium point here will always be  $P_-$ . We note that, in Sections 3.1 through 3.4 below, we will discuss in detail the various front propagation regimes that are realized in the cut-off Nagumo equation (2), as indicated already in Figure 3; the corresponding bifurcation structure of the vector field in (19) will be classified in Section 3.5.

Next, we determine the portion of the singular heteroclinic connection  $\Gamma$  that lies in this intermediate region. To that end, we note that the two hyperplanes  $\{u = 0\}$  and  $\{E = 0\}$  are invariant under the flow of (19). Since, in  $\{E = 0\}$ , these equations are equivalent to the first-order system (9), the existence of a singular solution follows from the fact that the

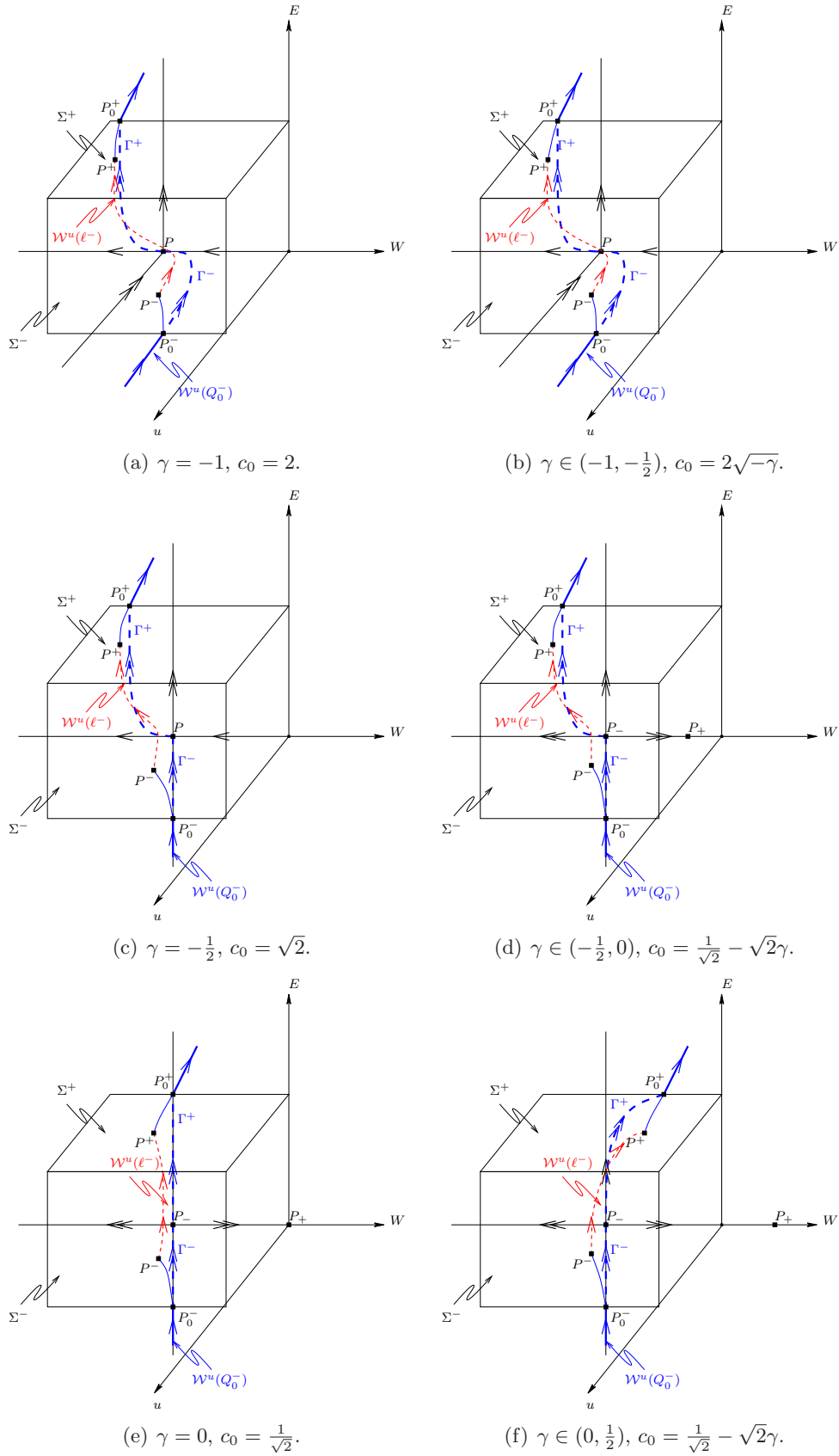


**Figure 3.** The geometry in the intermediate region in dependence of  $\gamma$  and  $c_0$ .

Nagumo equation supports traveling fronts in the absence of a cut-off for any  $\gamma \in [-1, \frac{1}{2})$ . Correspondingly, the portion of  $\Gamma$  that is located in  $\{E = 0\}$  is given by the equivalent of the segment  $\Gamma^-$ , as defined in Section 2.2, in  $(u, W, E)$ -coordinates. By contrast, for  $u = 0$ , we find the singular equation

$$\frac{dW}{dE} = \frac{c_0W + W^2 - \gamma}{EW}, \quad (20)$$

which is obtained by rewriting (19) with  $E$  as the independent variable. In particular, Equation (20) is separable and can hence be solved (in implicit form):

$$\ln E - \frac{1}{2} \ln |c_0W + W^2 - \gamma| - \frac{c_0}{\sqrt{4\gamma + c_0^2}} \operatorname{arctanh}\left(\frac{2W + c_0}{\sqrt{4\gamma + c_0^2}}\right) \equiv \text{constant}.$$

The corresponding orbit, which we denote by  $\Gamma^+$ , as in Section 2.3, determines the portion of the singular heteroclinic connection  $\Gamma$  that is located in  $\{u = 0\}$ .

For future reference, we note that the hyperplanes  $\Sigma^-$  and  $\Sigma^+$ , which were introduced in Sections 2.2 and 2.3, respectively, are given by

$$\begin{aligned} \Sigma^- &= \{(\rho, W, E) \mid (W, E) \in [-v_0, 0] \times [0, 1]\} \quad \text{and} \\ \Sigma^+ &= \{(u, W, 1) \mid (u, W) \in [0, \rho] \times [-v_0, 0]\} \end{aligned} \quad (21)$$

after transformation to phase-directional coordinates, as can be seen from (18) and the change of coordinates between the family chart and the phase-directional chart:

$$u = \varepsilon U, \quad W = \frac{V}{U}, \quad \text{and} \quad E = \frac{1}{U}. \quad (22)$$

(Here,  $\rho$  and  $v_0$  are defined as before.) Moreover, we remark that these two sections for the flow of (19) naturally separate the outer region from the intermediate region and the intermediate region from the inner region, respectively. Correspondingly, the respective points of intersection of  $\Gamma^-$  and  $\Gamma^+$  with  $\Sigma^-$  and  $\Sigma^+$  are given by the equivalents, in  $(u, W, E)$ -coordinates, of  $P_0^-$  and  $P_0^+$ , respectively, as defined in Sections 2.2 and 2.3.

In sum, the singular heteroclinic connection  $\Gamma$  is therefore given as the union of the orbits  $\Gamma^-$  and  $\Gamma^+$  and the singularities at  $Q_0^-$ ,  $P_-$ , and  $Q_0^+$ , which completes our discussion of the singular limit as  $\varepsilon \rightarrow 0^+$  in (8).

Finally, we recast the governing equations in this intermediate region in a form that is more convenient for the following analysis of the persistence of  $\Gamma$ : for  $\varepsilon \in (0, \varepsilon_0]$ , with  $\varepsilon_0$  positive and small, we first rewrite (19) in terms of the new variables  $Z = W + \frac{1}{2}c_0$  and  $c = c_0 + \Delta c$ :

$$u' = -(\frac{1}{2}c_0 - Z)u, \quad (23a)$$

$$Z' = (\frac{1}{2}c_0 - Z)\Delta c - Z^2 + \frac{1}{4}c_0^2 + \gamma - (1 + \gamma)u + u^2, \quad (23b)$$

$$E' = (\frac{1}{2}c_0 - Z)E. \quad (23c)$$

Then, we transform the resulting vector field by dividing out a factor of  $\frac{1}{2}c_0 - Z$  (which is positive in the  $Z$ -regime considered here, cf. Section 2.4) from the right-hand sides in (23):

$$u' = -u, \quad (24a)$$

$$Z' = \Delta c - \frac{Z^2 - (\frac{1}{4}c_0^2 + \gamma)}{\frac{1}{2}c_0 - Z} - \frac{(1 + \gamma)u - u^2}{\frac{1}{2}c_0 - Z}, \quad (24b)$$

$$E' = E. \quad (24c)$$

Since this last transformation corresponds to a rescaling of  $\xi$  that leaves the phase portrait of (23) unchanged, the prime now denotes differentiation with respect to some new independent variable  $\zeta$ . The transformed equations in (24) are the starting point for the geometric classification of front propagation in Equation (5) that is given in the following section.

### 3. Propagation regimes

In this section, we classify the propagation regimes (bistable, pushed, and pulled) that are realized in the cut-off Nagumo equation in dependence of the value of the control parameter  $\gamma \in [-1, \frac{1}{2})$ ; then, we discuss the boundary cases that limit these three ‘canonical’ regimes.

#### 3.1. Bistable regime

For  $\gamma \in (0, \frac{1}{2})$ , the Nagumo equation (2) (without cut-off) displays classical bistable reaction kinetics. It is well-known [1, 2] that a solution to the corresponding traveling front equation (6) is given by

$$u(\xi) = \frac{1}{1 + e^{\frac{1}{\sqrt{2}}(\xi - \xi^-)}}, \quad (25)$$

where  $\xi^- \geq 0$  denotes an arbitrary phase. That solution propagates between the stable rest states at 1 and 0, with propagation speed  $c^\dagger = \frac{1}{\sqrt{2}} - \sqrt{2}\gamma$ ; the corresponding orbit, in the context of the equivalent first-order system (8), is given by

$$v(u, c^\dagger) = \frac{1}{\sqrt{2}}u(u - 1), \quad (26)$$

as can be seen directly from (25). The reader is referred to [15] for details; in particular, we note that the relevant equilibrium point of the ‘projectivized’ dynamics in the intermediate region, which is governed by (19), is located at  $P_- = (0, -\frac{1}{\sqrt{2}}, 0)$ , as  $\frac{v}{u} = W \rightarrow -\frac{1}{\sqrt{2}}$  for  $u \rightarrow 0^+$ , by (18) and (26). (Correspondingly, the singular orbit  $\Gamma^-$ , which is defined by the equivalent, in  $(u, W, E)$ -coordinates, of (26), coincides with the stable manifold  $\mathcal{W}^s(P_-)$  of  $P_-$ .)

The effects of a cut-off in the bistable propagation regime were studied geometrically in [15], where it was proven that the cut-off Nagumo equation supports a traveling front solution for a unique value of  $c$ , with  $\varepsilon \in (0, \varepsilon_0]$  sufficiently small; cf. [15, Theorem 2.1]. (That value reduces to  $c^\dagger$  in the singular limit as  $\varepsilon \rightarrow 0^+$ .) In particular, it was shown there that the correction  $\Delta c(\varepsilon) = c - c^\dagger$  to the front propagation speed that is induced by the Heaviside cut-off  $H$  satisfies

$$\Delta c = \frac{\Gamma(4)}{\Gamma(1 + 2\gamma)\Gamma(3 - 2\gamma)} \frac{\sqrt{2}\gamma}{(1 + 2\gamma)^{2\gamma}} \varepsilon^{1+2\gamma} + o(\varepsilon^{1+2\gamma}) \equiv K_\gamma \varepsilon^{1+2\gamma} [1 + o(1)], \quad (27)$$

where  $\Gamma(\cdot)$  denotes the standard Gamma function [26, Section 6.1].

**Remark 6.** As observed in [15], the exponent of  $\varepsilon$  in the leading-order asymptotics of  $\Delta c$  is given by the ratio of two of the eigenvalues of the linearization of (19) at  $P_-$ . Specifically, for  $c_0 = c^\dagger$ , these eigenvalues evaluate to  $\frac{1}{\sqrt{2}}(1 + 2\gamma)$  and  $\frac{1}{\sqrt{2}}$ ; recall Table 3.  $\square$

The proof of these results, as given in [15], relies on a detailed analysis of the transition through the intermediate region under the flow of (24), and is performed entirely in the phase-directional chart. The crucial step in the argument, which is outlined below, consists in approximating the corresponding transition map between the two sections  $\Sigma^-$  and  $\Sigma^+$ ; cf. (21).

First, the equations in (24) are simplified via a (smooth, near-identity) normal form transformation [27] of the form  $\widehat{Z} = \widehat{Z}(u, Z) = Z + O(u)$ , which eliminates any  $u$ -dependence from (24b), whereas the dynamics of  $u$  and  $E$  remains unaffected:

$$\widehat{Z}' = \Delta c - \frac{\widehat{Z}^2 - [\frac{1}{4}(c^\dagger)^2 + \gamma]}{\frac{1}{2}c^\dagger - \widehat{Z}} = \Delta c - \frac{\widehat{Z}^2 - \frac{1}{8}(1 + 2\gamma)^2}{\frac{1}{2\sqrt{2}}(1 - 2\gamma) - \widehat{Z}}; \quad (28)$$

here, we have additionally substituted in  $c^\dagger = \frac{1}{\sqrt{2}} - \sqrt{2}\gamma$ . Next, we recall the definition of  $P^-$  and  $P^+$ , *i.e.*, of the points of intersection of  $\mathcal{W}^u(Q_\varepsilon^-)$  and  $\mathcal{W}^s(Q_\varepsilon^+)$  with  $\Sigma^-$  and  $\Sigma^+$ , respectively, from Sections 2.2 and 2.3. The points corresponding to  $P^-$  and  $P^+$ , after transformation to  $(u, \widehat{Z}, E)$ -variables, are labeled  $\widehat{P}^-$  and  $\widehat{P}^+$ , respectively.

**Remark 7.** We emphasize that the normal form transformation defined above removes the  $u$ -dependence in (24) to arbitrary order, as there is no resonance in the  $\gamma$ -regime considered here. In particular, the singular orbit  $\Gamma^-$  is rectified by that transformation, and is given by  $\widehat{Z}^- = -\frac{1}{2\sqrt{2}}(1 + 2\gamma)$ .  $\square$

Equation (28) is separable and can be integrated (in implicit form); the limits of integration in the resulting solution are fixed by the requirement that the point  $\widehat{P}^-$  is mapped to  $\widehat{P}^+$  in the transition through the intermediate region, *i.e.*, between  $\Sigma^-$  and  $\Sigma^+$ , under the flow of (28). The corresponding  $\zeta$ -values can be found as follows: since (28) is autonomous, we can, without loss of generality, set  $\zeta^- = 0$ . To determine  $\zeta^+ = -\ln \frac{\varepsilon}{\rho}$ , we solve (24a) exactly, noting that  $u$  evaluates to  $\rho$  and  $\varepsilon$  in  $\Sigma^-$  and  $\Sigma^+$ , respectively; recall (13) and (17). In sum, we find [15, Proposition 2.2]

$$\begin{aligned} & -\ln \frac{\varepsilon}{\rho} - \frac{1}{2} \ln \left| 2\widehat{Z}^2 + 2\Delta c\widehat{Z} - \frac{1}{\sqrt{2}}(1 - 2\gamma)\Delta c - \frac{1}{4}(1 + 2\gamma)^2 \right| \Big|_{\widehat{Z}^-}^{\widehat{Z}^+} \\ & - \frac{\frac{1}{\sqrt{2}}(1 - 2\gamma) + \Delta c}{\sqrt{\frac{1}{2}(1 + 2\gamma)^2 + \sqrt{2}(1 - 2\gamma)\Delta c + (\Delta c)^2}} \\ & \times \operatorname{arctanh} \left( \frac{2\widehat{Z} + \Delta c}{\sqrt{\frac{1}{2}(1 + 2\gamma)^2 + \sqrt{2}(1 - 2\gamma)\Delta c + (\Delta c)^2}} \right) \Big|_{\widehat{Z}^-}^{\widehat{Z}^+} = 0; \quad (29) \end{aligned}$$

by construction, the relation in (29) yields a necessary condition on the parameter  $\Delta c (= c - c^\dagger)$  for a connection between the two points  $\widehat{P}^-$  and  $\widehat{P}^+$  to persist, for  $\varepsilon \in (0, \varepsilon_0]$  positive and small.

It remains to obtain estimates for the respective  $\widehat{Z}$ -coordinates  $\widehat{Z}^-$  and  $\widehat{Z}^+$  of these points that are sufficiently accurate to the order considered here. To that end, one has to account for the global dynamics in the outer and inner regions, respectively, *i.e.*, one needs to expand the manifolds  $\mathcal{W}^u(Q_\varepsilon^-)$  and  $\mathcal{W}^s(Q_\varepsilon^+)$  introduced in Sections 2.2 and 2.3 to the corresponding order.

Thus, given  $v(u, c^\dagger)$ , as defined in (26), the  $v$ -coordinate of  $P^-$  (in the outer region) satisfies  $v^- = -\frac{1}{\sqrt{2}}\rho(\rho - 1) + O(\Delta c)$ ; cf. the expansion in (10). Here, the  $O(\Delta c)$ -terms can be evaluated exactly due to the fact that a traveling front solution for (5) is known in the absence of a cut-off, as well as that the solution of the variational equation (12) along the corresponding orbit of (9) can also be determined in closed form in this case: with  $v(u, c^\dagger)$  as before, that equation reduces to

$$\frac{\partial}{\partial u} \left( \frac{\partial v}{\partial c}(u, c^\dagger) \right) = -1 + 2 \frac{u - \gamma}{u(1 - u)} \frac{\partial v}{\partial c}(u, c^\dagger). \quad (30)$$

Equation (30) can be solved by variation of constants, which gives

$$\frac{\partial v}{\partial c}(u, c^\dagger) = \frac{1}{3 - 2\gamma} u^{-2\gamma} (1 - u) F(3 - 2\gamma, -2\gamma; 4 - 2\gamma; 1 - u) \quad (31)$$

for the unique solution satisfying the boundary condition  $\frac{\partial v}{\partial c}(1, c^\dagger) = 0$ ; cf. [15, Lemma 2.2]. (Here,  $F(\cdot, \cdot; \cdot; \cdot)$  denotes the hypergeometric function; see *e.g.* [26, Section 15].)

Similarly, in the inner region, the  $v$ -coordinate  $v^+$  of  $P^+$  can be determined from the corresponding solution of (15) with  $V(0) = 0$ : since, clearly,  $V(U) = -cU$ , it follows that  $v(u) = -cu$  and, hence, that  $v^+ = -c = -c^\dagger - \Delta c$  after ‘blow-down,’ *i.e.* in the original  $(u, v, \varepsilon)$ -variables; cf. (14).

Consequently, after application of the normal form transformation defined above, it follows that  $\widehat{Z}^-$  and  $\widehat{Z}^+$  can be estimated as

$$\begin{aligned}\widehat{Z}^-(\rho, \Delta c) &= -\frac{1}{2\sqrt{2}}(1 + 2\gamma) + \frac{1}{\rho^{1+2\gamma}} \frac{\Gamma(1 + 2\gamma)\Gamma(3 - 2\gamma)}{\Gamma(4)} [1 + o(1)] \quad \text{and} \\ \widehat{Z}^+(\Delta c, \varepsilon) &= -\frac{1}{2\sqrt{2}}(1 - 2\gamma) - \Delta c [1 + o(1)];\end{aligned}\tag{32}$$

see [15, Lemmas 2.2 and 2.4]. (Here,  $o(1)$  denotes higher-order terms in  $\rho$ ,  $\Delta c$ , and  $\varepsilon$ .)

Substituting (32) into (29), expanding the result in terms of  $\Delta c$  and  $\varepsilon$  and applying the Implicit Function Theorem at  $(\Delta c, \varepsilon) = (0, 0)$ , one can show that the (unique) value of  $\Delta c = \Delta c(\varepsilon, \gamma)$  for which  $\Gamma$  persists is indeed well-defined; moreover, the persistence proof sketched above also yields the leading-order  $\varepsilon$ -asymptotics of  $\Delta c$ , cf. (27), as can be seen by solving the corresponding relation that is obtained from (29) to leading order. Finally, since the persistent heteroclinic connection between  $Q_\varepsilon^-$  and  $Q_\varepsilon^+$  that is realized for  $c = c^\dagger + \Delta c(\varepsilon)$  in (8) corresponds to a traveling front solution of the cut-off Nagumo equation (5), the existence and uniqueness of such fronts in this bistable regime follows.

### 3.2. Pushed regime

When  $\gamma \in (-\frac{1}{2}, 0)$ , Equation (2) supports pushed fronts in the absence of a cut-off, as outlined in the Introduction. The corresponding propagation speed is again given by  $c^\dagger = \frac{1}{\sqrt{2}} - \sqrt{2}\gamma$  [2], as in the bistable regime considered in Section 3.1. (We note that, for  $\gamma \in (-\frac{1}{2}, 0)$ , that speed is higher than the speed  $c^* = 2\sqrt{-\gamma}$  that is predicted by linearization at the zero rest state, in accordance with the definition of pushed traveling fronts [3].)

Results obtained previously in this pushed regime [4], which relied on a modification of the integral variational principle developed by Benguria and Depassier [3], indicate that the correction to  $c^\dagger$  that is due to the Heaviside cut-off  $H$  in (6) is again given by (27), as was the case in the bistable regime.

This expectation is confirmed by our geometric analysis of the first-order system (8) for  $\gamma \in (-\frac{1}{2}, 0)$ ; a rigorous, in-depth discussion of pushed front propagation in the cut-off Nagumo equation will be given in the upcoming article [16]. In particular, it is shown there that the existence and uniqueness analysis developed in [15], for the bistable regime, remains mostly valid in the pushed regime, *i.e.*, that only minor modifications are required. Thus, the singular orbit  $\Gamma$  can be constructed exactly as before; moreover, the proof of persistence of that orbit for  $\varepsilon \in (0, \varepsilon_0]$  positive and small remains valid when  $\gamma \in (-\frac{1}{2}, 0)$ . Specifically, the  $Z$ -dynamics in the intermediate region is still governed by the normal form equation (28); see Section 2.4 above. (In particular, we remark that the eigenvalues of the linearization about the relevant equilibrium point  $P_-$  are again not in resonance.) Correspondingly, the argument presented in [15, Section 3], and outlined in Section 3.1, carries over almost verbatim to the pushed regime.

Finally, we remark that the correction  $\Delta c$  to  $c^\dagger$  that is due to the cut-off  $H$  in (5) is negative in this regime, as is evident from (27) with  $\gamma \in (-\frac{1}{2}, 0)$ , which contrasts with the bistable regime and is in agreement with the general observation made in the Introduction that cut-offs reduce the propagation speed of pushed fronts; see also [15, 16, 20, 21].

### 3.3. Pulled regime

In the pulled regime, with  $\gamma \in (-1, -\frac{1}{2})$ , the propagation speed of traveling fronts in the absence of a cut-off is determined by linearization of Equation (2) at the zero rest state:  $c^* = 2\sqrt{-\gamma}$ .

To find the correction  $\Delta c = c - c^*$  that is induced by a Heaviside cut-off in (5) in this regime, one could proceed as in Sections 3.1 and 3.2. In particular, the dynamics in the outer region is again governed by the corresponding traveling front equation without cut-off, or, equivalently, by the first-order system (9); in contrast to the bistable and pushed regimes, however, no exact expression seems to be available for the traveling front solution that propagates between the rest states at 1 and 0 in this case. The governing equations in the inner region, where the flow of (8) is cut-off, are given by (15), as before, since the corresponding reaction terms are canceled by the Heaviside cut-off  $H$ . In the intermediate region, Equation (19b) reduces to

$$Z' = \Delta c - \frac{Z^2}{\sqrt{-\gamma} - Z} - \frac{(1 + \gamma)u - u^2}{\sqrt{-\gamma} - Z}, \quad (33)$$

after transformation to the new variables  $Z = W + \sqrt{-\gamma}$  ( $= W + \frac{1}{2}c^*$ ) and  $c = 2\sqrt{-\gamma} + \Delta c$  ( $= c^* + \Delta c$ ). Here, we note that there exists only one relevant equilibrium point in this pulled regime, since  $P_- = P_+$  for  $c = c^*$  in (19). We denote that point by  $P$ , and we remark that  $P$  corresponds to the one eigendirection of the linearization of (9) at  $Q_0^+$ , which is a degenerate node now; recall Table 2. Finally, the relevant normal form equation is given by  $\widehat{Z}' = \Delta c - \frac{\widehat{Z}^2}{\sqrt{-\gamma} - \widehat{Z}}$ ; see also [6, Equation (34b)]. (In particular, comparing this equation to the general normal form in (28), one finds that the constant term cancels.) The associated transition map  $\Pi$  from  $\Sigma^-$  to  $\Sigma^+$  can then be approximated to leading order, as was done in the proof of [6, Proposition 3.2].

**Remark 8.** As the eigenvalues of the linearization of (19) about  $P$  are given by  $-\sqrt{-\gamma}$ , 0, and  $\sqrt{-\gamma}$  in this regime, recall Tables 3 and 4, they are clearly in resonance. However, since none of the  $u$ -dependent terms in (33) are resonant, those terms can still be eliminated by a standard normal form transformation, as in [6, Proposition 3.2].  $\square$

Instead of studying the pulled propagation regime in (2) directly, as outlined above, we take an alternative approach here: we show that, for  $\gamma \in (-1, -\frac{1}{2})$ , the cut-off Nagumo equation (5) is equivalent to an FKPP-type equation, which was analyzed geometrically in [6]. In particular, for the FKPP equation proper, with  $f(\phi) = \phi(1 - \phi)$  in (1), it was proven there that the correction  $\Delta c$  to the front propagation speed  $c^*$  that is due to a cut-off is given by

$$\Delta c(\varepsilon) = -\frac{\pi^2}{(\ln \varepsilon)^2} + o[(\ln \varepsilon)^{-2}] \equiv \frac{K_{-1}}{(\ln \varepsilon)^2} [1 + o(1)], \quad (34)$$

in accordance with a conjecture made previously by Brunet and Derrida [5]; see the Introduction and [6] for details. Moreover, in Section 4 of that article, it was shown that the leading-order asymptotics in (34) remains valid for more general cut-off equations of the type

$$\frac{\partial \phi}{\partial t} = \frac{\partial^2 \phi}{\partial x^2} + [\phi - g(\phi)]H(\phi - \varepsilon), \quad (35)$$

where  $H$  is as defined in (4) and the function  $g$  satisfies the following assumptions:

- (i)  $g(\phi) = O(\phi^2)$  as  $\phi \rightarrow 0^+$ ,
- (ii) there exists a  $\phi^- > 0$  such that  $g(\phi^-) = \phi^-$ ,
- (iii)  $g'(\phi^-) > 1$ , and
- (iv)  $0 < g(\phi) < \phi$  for all  $\phi \in (0, \phi^-)$ .

(The above conditions ensure that zero is again a rest state of the traveling front equation  $u'' + cu' + [u - g(u)]H(u - \varepsilon) = 0$  that is associated with (35), as well as that the rest state at  $\phi^-$  corresponds to a hyperbolic saddle equilibrium of that same equation. In particular, the condition in (iv) implies that there exist no other equilibria, as well as that a trapping region can be constructed for the flow of the corresponding vector field in the intermediate region.)

The following is the main result of this section (and, indeed, of this article):

**Proposition 1.** For  $\gamma \in (-1, -\frac{1}{2})$  and  $\varepsilon \in (0, \varepsilon_0]$ , Equation (5) supports a unique traveling front solution propagating between the rest states at 1 and 0. Moreover, the corresponding propagation speed  $c$  can be written as  $c = c^* + \Delta c(\varepsilon)$ , where  $c^* = 2\sqrt{-\gamma}$  and

$$\Delta c(\varepsilon) = -\frac{\pi^2 \sqrt{-\gamma}}{(\ln \varepsilon)^2} + o[(\ln \varepsilon)^{-2}] \equiv \frac{K_\gamma}{(\ln \varepsilon)^2} [1 + o(1)]. \quad (36)$$

To transform the cut-off Nagumo equation (5) into the framework of [6, Section 4], we first rewrite the corresponding traveling front equation (6) as

$$u'' + cu' - \gamma \left( u - \frac{\gamma+1}{\gamma} u^2 + \frac{1}{\gamma} u^3 \right) H(u - \varepsilon) = 0; \quad (37)$$

then, we introduce the new variable  $\Xi = \sqrt{-\gamma}\xi$  in (37). Finally, rescaling the front propagation speed  $c$  via  $c = \sqrt{-\gamma}C$ , we obtain

$$\ddot{u} + C\dot{u} + \left[ u - \left( \frac{\gamma+1}{\gamma} u^2 - \frac{1}{\gamma} u^3 \right) \right] H(u - \varepsilon) = 0, \quad (38)$$

where overdots denote differentiation with respect to  $\Xi$ .

**Remark 9.** Alternatively, instead of rescaling  $\xi$ , we could have rescaled time and space in the original reaction-diffusion equation (5) via  $T = -\gamma t$  and  $X = \sqrt{-\gamma}x$ , which would have given  $\Xi = X - CT = \sqrt{-\gamma}(x - \sqrt{-\gamma}Ct) = \sqrt{-\gamma}\xi$ , as before.  $\square$

Defining  $g(u) = \frac{\gamma+1}{\gamma}u^2 - \frac{1}{\gamma}u^3$ , one sees that the transformed Equation (37) satisfies the conditions in (i), (ii), and (iii) above, with  $\phi^- = 1$ . Hence, it only remains to verify the condition in (iv): however, while  $g(u) < u$  is certainly satisfied, *i.e.*, while (37) has no rest states in the (open) interval  $(0, 1)$ , as the roots of  $g(u) = u$  are located at  $\gamma$ , 0, and 1, the condition that  $g$  is non-negative on that interval does not hold for  $\gamma > -1$ . The latter condition is imposed in [6, Section 4] to ensure the existence of a trapping region for the flow in the intermediate region which, in turn, guarantees the existence of a singular heteroclinic connection  $\Gamma$  in that region. Nevertheless, we can construct such a trapping region explicitly here; the corresponding argument is analogous to that given in the proof of [6, Lemma 2.5], and is based on a phase plane analysis of the first-order system

$$\dot{u} = v, \quad (39a)$$

$$\dot{v} = -2v - \left[ u - \left( \frac{\gamma+1}{\gamma} u^2 - \frac{1}{\gamma} u^3 \right) \right] \quad (39b)$$

that is obtained from (38) for  $\varepsilon = 0$ , *i.e.*, in the absence of a cut-off. (Here, we note that the singular front propagation speed  $C_0$  is given by  $C^* = 2$  now.)

**Lemma 1.** For  $\gamma \in (-1, -\frac{1}{2})$  and  $u \in (0, \rho)$ , with  $\rho \geq \varepsilon_0$  as in (21), the flow of (39) is trapped in the wedge that is bounded by  $\{v = 0\}$  and  $\{v = -u - \frac{\gamma+1}{\gamma}u^2\}$ .

*Proof.* Evaluating the right-hand sides in (39) for  $v = 0$ , we find

$$(0, 1) \cdot \left( 0, -u + \frac{\gamma+1}{\gamma}u^2 - \frac{1}{\gamma}u^3 \right)^T = -u \left( 1 - \frac{\gamma+1}{\gamma}u + \frac{1}{\gamma}u^2 \right),$$

which is negative when  $\gamma \in (-1, -\frac{1}{2})$  and  $u \in (0, 1)$ . Similarly, for  $v = -u - \frac{\gamma+1}{\gamma}u^2$ , the corresponding expression is given by

$$\left( 1 + 2\frac{\gamma+1}{\gamma}u, 1 \right) \cdot \left( -u - \frac{\gamma+1}{\gamma}u^2, u + 3\frac{\gamma+1}{\gamma}u^2 - \frac{1}{\gamma}u^3 \right)^T = -u^3 \left[ 2\left( \frac{\gamma+1}{\gamma} \right)^2 + \frac{1}{\gamma} \right], \quad (40)$$

which is positive in that same  $(\gamma, u)$ -regime. Hence, a trapping region for (39) is defined by  $\{v = 0\}$  and  $\{v = -u - \frac{\gamma+1}{\gamma}u^2\}$ .

It remains to show that the flow of (39) actually enters the region that is bounded by these two curves and, hence, that it has to remain trapped there. Now, the origin  $Q_0^+$  is a degenerate node for (39), with a strong stable manifold  $\mathcal{W}^{ss}(Q_0^+)$  that satisfies  $v(u) = -u - \frac{\gamma+1}{\gamma}u^2 + [\frac{1}{2\gamma} + (\frac{\gamma+1}{\gamma})^2]u^3 + O(u^4)$ . Denoting the point of intersection of that manifold with the section  $\Sigma^-$  defined in (21) by  $P_0^{ss}$  and taking into account that  $[\frac{1}{2\gamma} + (\frac{\gamma+1}{\gamma})^2]$  is negative for  $\gamma \in (-1, -\frac{1}{2})$ , we find  $v_0^{ss} < -[1 + \frac{\gamma+1}{\gamma}\rho]\rho$  for the  $v$ -coordinate of  $P_0^{ss}$ . Since  $\mathcal{W}^{ss}(Q_0^+)$  coincides with the stable manifold of the equilibrium point  $P = (0, -1, 0)$  for

$$\dot{u} = uW, \tag{41a}$$

$$\dot{W} = -2W - W^2 - \left[1 - \left(\frac{\gamma+1}{\gamma}u - \frac{1}{\gamma}u^2\right)\right], \tag{41b}$$

$$\dot{E} = -EW, \tag{41c}$$

after transformation of (39) to  $(u, W, E)$ -coordinates, we conclude as in [6, Lemma 2.5] that the segment  $\Gamma^-$  of the singular heteroclinic orbit  $\Gamma$ , which is located in the outer region and which corresponds precisely to the unstable manifold  $\mathcal{W}^u(Q_0^-)$  of  $Q_0^-$ , has to enter the trapping region constructed above, which completes the proof.  $\square$

**Remark 10.** The definition of the trapping region in Lemma 1 is motivated by the fact that the linearization of (41) in the  $(u, W)$ -plane about  $P$  has eigenvectors  $(0, 1, 0)^T$  and  $(1, -\frac{\gamma+1}{\gamma}, 0)^T$ , from which the curves bounding that region can easily be obtained.  $\square$

**Remark 11.** The proof of Lemma 1 implies, in particular, that the singular orbit  $\Gamma^-$  must be tangent to the  $W$ -axis as  $\Gamma^- \rightarrow P$  in the intermediate region; see also [6, Lemma 2.5]. Specifically, for  $E = 0$ , the flow of (41) is trapped in the wedge that is bounded by the  $u$ -axis  $\{W = 0\}$  and the curve defined by  $\{W = -1 - \frac{\gamma+1}{\gamma}u\}$ . Moreover, when  $\gamma \in (-1, -\frac{1}{2})$ , the equivalents  $W_0^{ss}$  and  $W_0^-$  of  $v_0^{ss}$  and  $v_0^-$  (the  $W$ -coordinates of the points of intersection of  $\mathcal{W}^{ss}(Q_0^+)$  and  $\Gamma^-$ , respectively, with  $\Sigma^-$ ) must satisfy  $W_0^- > W_0^{ss}$ . Since the relevant eigenvalues of the linearization of (41) at  $P$  are given by  $-1$  and  $0$ , the statement follows.  $\square$

In sum, we conclude that the results of [6, Section 4] can be applied to the rescaled Nagumo equation (5) (with cut-off) in this pulled propagation regime. In particular, it follows that, for  $\gamma \in (-1, -\frac{1}{2})$  and  $\varepsilon \in (0, \varepsilon_0]$  sufficiently small, Equation (38) supports a unique traveling front solution that propagates between the rest states at 1 and 0, with speed

$$C = C^* + \Delta C(\varepsilon) = 2 - \frac{\pi^2}{(\ln \varepsilon)^2} + o[(\ln \varepsilon)^{-2}].$$

Recalling  $c = \sqrt{-\gamma}C$ , we obtain (36), as claimed, which completes the proof of Proposition 1.

### 3.4. Boundary cases

In this section, we study the cut-off Nagumo equation (5) for the three values  $-1$ ,  $-\frac{1}{2}$ , and  $0$  of  $\gamma$  that bound the open intervals  $(-1, -\frac{1}{2})$ ,  $(-\frac{1}{2}, 0)$ , and  $(0, \frac{1}{2})$  corresponding to the pulled, pushed, and bistable front propagation regimes, respectively, discussed in Sections 3.1 through 3.3 above. In particular, we show that the dynamics of (8) in one of these boundary cases is complicated by the occurrence of resonances in the rescaled equations that describe the dynamics in the intermediate region, *i.e.*, in phase-directional coordinates.

*3.4.1. Case 1:  $\gamma = -1$*  For  $\gamma = -1$ , Equation (5) corresponds precisely to the classical Kolmogorov-Petrovskii-Piscounov (KPP) equation discussed in [6], with reaction terms  $f(\phi) = \phi(1 - \phi^2)$ . (Alternatively, that equation goes by the name Newell-Whitehead equation [22].) In particular, the trapping region constructed in Lemma 1 coincides with the corresponding region that was found in [6, Lemma 2.5] in this case. Hence, the result of Proposition 1 remains valid, and is an immediate consequence of [6, Theorem 1.1] now; correspondingly, the correction  $\Delta c$  to the linear spreading speed  $c^*$  that is due to the cut-off is again given by (34).

*3.4.2. Case 2:  $\gamma = -\frac{1}{2}$*  The case where  $\gamma = -\frac{1}{2}$  separates the pushed and pulled propagation regimes, and can be analyzed via an adaptation of the analysis developed in [6] and [15]; recall our discussion of the corresponding regimes in Sections 3.2 and 3.3 above.

As before, the conditions in (i), (ii), and (iii) imposed in that section will hold in this case, as well, whereas (iv) will again fail. However, the proof of Lemma 1 will no longer yield a trapping region for the flow of the transformed first-order system (39), as the expression in (40) will evaluate to zero when  $\gamma = -\frac{1}{2}$ . Hence, the results of [6, Section 4] are not applicable here. Nevertheless, we can still prove an analogue of Proposition 1, as follows: first, we note that the unique connection between  $Q_0^-$  and  $Q_0^+$  in (9), in the absence of a cut-off, can be found in closed form, with  $v(u, \sqrt{2})$  as defined in (26). (The front propagation speed is given by  $c_0 = \sqrt{2}$  now; in particular, the linear spreading speed  $c^* = 2\sqrt{-\gamma}$  equals  $c^\dagger = \frac{1}{\sqrt{2}} - \sqrt{2}\gamma$  when  $\gamma = -\frac{1}{2}$ .) Hence, the singular orbit  $\Gamma^-$  is again known explicitly, and is given by  $W(u) = \frac{1}{\sqrt{2}}(u - 1)$ , after transformation to  $(u, W, E)$ -coordinates; recall (18). Since the singular equations that are obtained from (19) for  $u = 0$ , *i.e.*, in the  $(W, E)$ -plane, can be solved exactly, as in [6, Section 2.1], one can show that the segment of  $\Gamma^+$  that is located in this intermediate region can be found in terms of the so-called Lambert W-function [28]. In sum, it follows that a singular heteroclinic  $\Gamma$  can be constructed as in [6, Section 2.1].

Therefore, it only remains to prove that  $\Gamma$  will persist as a heteroclinic connection between  $Q_\varepsilon^-$  and  $Q_\varepsilon^+$ , for  $\varepsilon$  positive and sufficiently small and a unique value of  $c$  in (8). The required persistence argument follows the discussion in Sections 3.1 and 3.2, and will only be outlined here; cf. also the proof of [6, Proposition 3.1].

First, we note that the normal form equation for  $\widehat{Z}$  and the resulting (implicit-form) solution are again given by (28) and (29), respectively, with  $\gamma$  there replaced by  $-\frac{1}{2}$  here. (Thus, the equations governing the dynamics in the intermediate region, as found in the bistable and pushed regimes, are still valid in this boundary case.) Similarly, the solution of the variational equation (30) can be determined in closed form, as before:

$$\frac{\partial v}{\partial c}(u, \sqrt{2}) = \frac{u}{(u-1)^3} \left( -\frac{1}{3}u^3 + \frac{3}{2}u^2 - 3u + \ln u + \frac{11}{6} \right) = u \left( -\frac{11}{6} - \ln u \right) + O(u^2 \ln u).$$

Correspondingly, estimates for the respective  $\widehat{Z}$ -coordinates of  $\widehat{P}^-$  and  $\widehat{P}^+$  are given by

$$\widehat{Z}^-(\rho, \Delta c) = -\frac{11}{6}\Delta c[1 + o(1)] \quad \text{and} \quad \widehat{Z}^+(\Delta c, \varepsilon) = -\frac{1}{\sqrt{2}} - \Delta c[1 + o(1)] \quad (42)$$

now; recall the discussion in Section 3.1 and, in particular, (32). (Here,  $o(1)$  denotes higher-order terms in  $\rho$ ,  $\Delta c$ , and  $\varepsilon$ , as above.) Substituting (42) into (29), expanding the result in terms of  $\Delta c$  and  $\varepsilon$ , recalling that  $\zeta^+ = -\ln \frac{\varepsilon}{\rho}$ , and taking into account that  $\Delta c$  is once again negative, we have

$$-\ln \frac{\varepsilon}{\rho} - \frac{1}{2} \ln |-1 + o(1)| + \frac{1}{2} \ln |\sqrt{2}\Delta c[1 + o(1)]| - \frac{1}{\sqrt[4]{2}\sqrt{-\Delta c}} \left\{ \frac{\pi}{2} - \frac{7}{3} \sqrt[4]{2}\sqrt{-\Delta c}[1 + o(1)] \right\} = 0. \quad (43)$$

Retaining only the leading-order terms in (43), we find that  $\Delta c$  must necessarily satisfy

$$\sqrt{-\Delta c}(-\ln \varepsilon + \ln \sqrt{-\Delta c}) = -\frac{\pi}{2\sqrt[4]{2}}[1 + o(1)].$$

Solving this relation to lowest order in  $\Delta c$  and  $\varepsilon$  and noting that the solution can again be written in terms of the Lambert W-function, we obtain  $\sqrt{-\Delta c} = \frac{\pi}{2\sqrt[4]{2}}(\ln \varepsilon)^{-1}[1 + o(1)]$ . In sum, it follows that the result of Proposition 1 carries over almost verbatim to this case; however, while the leading-order asymptotics of  $\Delta c(\varepsilon) = c - c^*$  is again logarithmic in  $\varepsilon$ , as in (36), the corresponding coefficient differs by a factor of  $\frac{1}{4}$  now:

$$\Delta c(\varepsilon) = -\frac{\pi^2}{4\sqrt{2}(\ln \varepsilon)^2} + o[(\ln \varepsilon)^{-2}] \equiv \frac{K_{-\frac{1}{2}}}{(\ln \varepsilon)^2}[1 + o(1)]. \quad (44)$$

**Remark 12.** The discrepancy between the leading-order asymptotics of  $\Delta c$ , as stated in (44), and the expression obtained by evaluating (36) for  $\gamma \rightarrow -\frac{1}{2}^-$  is due to  $\widehat{Z}^- = O(\Delta c)$ ; recall (42). Since the argument in the proof of [6, Proposition 3.1] assumes  $\widehat{Z}^- = O(1)$  (in our notation), the results of [6, Section 4] no longer apply when  $\gamma = -\frac{1}{2}$ .  $\square$

*3.4.3. Case 3:  $\gamma = 0$*  For  $\gamma = 0$ , Equation (2) reduces to the so-called Zeldovich equation, which is also known as the Huxley equation, see *e.g.* [1] or [22]. The corresponding cut-off equation was analyzed in detail in [20], where it was shown that the correction  $\Delta c$  to the front propagation speed  $c_0 = \frac{1}{\sqrt{2}}$  that is induced by a Heaviside cut-off is given by

$$\Delta c(\varepsilon) = -\frac{3}{\sqrt{2}}\varepsilon^2 + o(\varepsilon^2) \equiv K_0\varepsilon^2[1 + o(1)], \quad (45)$$

to leading order in  $\varepsilon$ . The proof of (45) is based on the same geometric framework that was introduced in Section 2 above; however, the analysis of the flow in the intermediate region is complicated by the occurrence of resonances between the eigenvalues of the linearization of the vector field in (19) at  $P_-$ . Specifically, it follows from standard theory [27] that the corresponding  $u$ -dependent terms are resonant; hence, they cannot be removed via a normal form transformation, as was the case in the canonical propagation regimes (pulled, pushed, and bistable) discussed above; rather, these terms give rise to logarithmic (‘switchback’) terms (in  $\varepsilon$ ) in the transition through the intermediate region. Correspondingly, the expansion for  $\Delta c$  in (45) will contain an  $O(\varepsilon^4 \ln \varepsilon)$ -term, as well as higher-order terms of the form  $\varepsilon^j (\ln \varepsilon)^k$ , with  $j \geq k$  and  $j \geq 4$  [20]. In particular, while the restriction of the unstable manifold  $\mathcal{W}^u(Q_\varepsilon^-)$  of  $Q_\varepsilon^-$  to the outer region is analytic in  $c$  and  $\varepsilon$ , the logarithmic dependence of  $\Delta c$  on  $\varepsilon$  gives rise to switchback terms in the expansion for  $v(u, c)$  in (10), resulting in a loss of smoothness when that expansion is considered in terms of  $\varepsilon$  alone; see [20, Section 5] for details. For a more general discussion of logarithmic switchback from a geometric point of view, the reader is referred to [29].

### 3.5. Classification

Given our discussion of the various propagation regimes that can be realized in the cut-off Nagumo equation (5) in dependence of  $\gamma$ , see Sections 3.1 through 3.4, we now combine the asymptotics obtained separately in these regimes to arrive at a comprehensive geometric classification of the global front propagation dynamics of (5). In fact, the equivalence of the traveling wave equation (6) and the first-order system (8) allows for such a classification in terms of the local flow about the origin  $Q_0^+$ : in the absence of a cut-off, that point is a hyperbolic

saddle equilibrium for (8) in the bistable propagation regime, when  $\gamma \in (0, \frac{1}{2})$ , while it becomes a proper (stable) node if  $\gamma \in (-\frac{1}{2}, 0)$  and a degenerate stable node for  $\gamma \in [-1, -\frac{1}{2}]$ , *i.e.*, in the pushed and pulled regimes, respectively; cf. Table 2. (In particular, we find that  $Q_0^+$  undergoes a saddle-node bifurcation at  $\gamma = 0$ .)

This transition from a hyperbolic saddle via a regular node to a degenerate node is reflected in the dynamics of the governing equations that are obtained from (8) in phase-directional coordinates (after blow-up). Thus, a crucial step in our analysis consists in the accurate description of the flow in the corresponding intermediate region. (Here, we recall that the cut-off equations in (8) reduce to (9) in that region, as the dynamics is unaffected by the cut-off there.) In particular, it follows that front propagation in the cut-off Nagumo equation is classifiable in terms of the normal form system that corresponds to the equations in (19), after removal of any non-resonant (higher-order) terms. The resulting dynamics is determined by the parameter  $\gamma$  and the front propagation speed  $c_0$  that is realized in the absence of a cut-off, as illustrated in Figure 3. Recalling that the equilibrium points  $P_- = (0, \lambda_-^+, 0)$  and  $P_+ = (0, \lambda_+^+, 0)$  for (19) correspond to the two eigendirections of the linearization of the equivalent first-order system (9) about  $Q_0^+$ , see Section 2.4, we can classify the flow in the intermediate region as follows.

When  $\gamma \in (0, \frac{1}{2})$ , *i.e.*, when  $Q_0^+$  is a hyperbolic saddle, the unique decaying mode of that linearization is given by  $P_-$ , since  $\lambda_-^+ < 0 < \lambda_+^+$ ; similarly, for  $\gamma \in (-\frac{1}{2}, 0)$ , the stronger decay rate at the node  $Q_0^+$  corresponds to  $P_-$ , as  $\lambda_-^+ < \lambda_+^+ < 0$  then. The relevant front propagation speed  $c^\dagger$  exceeds the linear spreading speed  $c^*$  in these two regimes. Finally, when  $\gamma = 0$ ,  $P_+$  lies at the origin, as  $\lambda_+^+$  evaluates to zero; hence,  $P_-$  corresponds to the unique strongly decaying mode at the saddle-node  $Q_0^+$ , while the front propagation speed is still given by  $c^\dagger$ .

Now, if  $c^\dagger$  remained the selected speed for  $\gamma \in [-1, -\frac{1}{2}]$ , the points  $P_-$  and  $P_+$  would pass through each other and exchange position, *i.e.*, the stronger rate of decay would be given by  $P_+$  in that scenario. Since, however, the  $Z$ -direction would then become attracting for  $P_-$ , cf. Table 3, while the  $Z$ -coordinates of  $P^-$  and  $P^+$  (the points of intersection of  $\mathcal{W}^u(Q_\varepsilon^-)$  and  $\mathcal{W}^s(Q_\varepsilon^+)$  with  $\Sigma^-$  and  $\Sigma^+$ , respectively) would still satisfy  $Z^- > Z^+$ , recall Section 3.1 and, in particular, (32), it would follow by continuity that no connection between  $P^-$  and  $P^+$  would be possible. (A similar argument can be found in [25], where the correction  $\Delta c$  in the bistable Schlögl equation [1] was shown to be negative, via phase space considerations.)

Consequently, the cut-off traveling front equation (6) would have no solution for any  $\varepsilon \in (0, \varepsilon_0]$  if  $c^\dagger$  was the relevant front propagation speed when  $\gamma \in [-1, -\frac{1}{2}]$ ; rather, the traveling front must select the lower speed  $c^*$  then. (To state it differently, solvability of (6) is maintained by adjusting the propagation speed so that the dynamics in this intermediate region is ‘frozen’ at a degenerate node, with  $P_- = P_+$ .) For completeness, we note that  $c^\dagger$  equals  $c^*$  when  $\gamma = -\frac{1}{2}$ , *i.e.*, that no distinction has to be made between the two in that case; correspondingly, the two equilibria  $P_-$  and  $P_+$  collapse onto one point  $P$ , as the eigenvalues  $\lambda_-^+$  and  $\lambda_+^+$  coalesce.

A distinguishing characteristic of the dynamics in the intermediate region is the potential occurrence of resonances among the eigenvalues of the linearization of (19) about  $P_-$ . In particular, these resonances are realized in the pulled propagation regime, as zero is always an eigenvalue, while the remaining two eigenvalues are negatives of each other. Correspondingly, the  $\varepsilon$ -asymptotics of  $\Delta c$  contains logarithmic switchback terms [29, 30] of the form  $(\ln \varepsilon)^{-k}$ , with  $k \geq 2$ , in that regime; see also [31, 32], where such terms were reported in the context of the so-called Lagerstrom model problem from fluid dynamics [30]. However, the corresponding normal form equations are simpler than those found in the boundary cases where  $\gamma = 0$  [20] or  $\gamma = \frac{1}{2}$  [21], see Section 3.4.3, and are in fact explicitly integrable; recall Section 3.3. Finally, we remark that no resonances occur in the bistable and pushed propagation regimes. Hence, any higher-order terms can be removed from the relevant normal form equations, as discussed in Sections 3.1 and 3.2; moreover,  $\Delta c$  is regular in  $\varepsilon$ , *i.e.*, no logarithmic switchback can occur

**Table 5.** Correction  $\Delta c$  to  $c_0$  due to a cut-off in (5) in dependence of  $\gamma$ .

| $\gamma$             | regime   | $c_0$                                 | $\Delta c$                   | $K_\gamma$  | sign     |
|----------------------|----------|---------------------------------------|------------------------------|---|----------|
| -1                   | pulled   | 2                                     | $O[(\ln \varepsilon)^{-2}]$  | $-\pi^2$  | negative |
| $(-1, -\frac{1}{2})$ | pulled   | $2\sqrt{-\gamma}$                     | $O[(\ln \varepsilon)^{-2}]$  | $-\sqrt{-\gamma}\pi^2$  | negative |
| $-\frac{1}{2}$       | pulled   | $\sqrt{2}$                            | $O[(\ln \varepsilon)^{-2}]$  | $-\frac{1}{4\sqrt{2}}\pi^2$   | negative |
| $(-\frac{1}{2}, 0)$  | pushed   | $\frac{1}{\sqrt{2}} - \sqrt{2}\gamma$ | $O(\varepsilon^{1+2\gamma})$ | $\frac{\Gamma(4)}{\Gamma(1+2\gamma)\Gamma(3-2\gamma)} \frac{\sqrt{2}\gamma}{(1+2\gamma)^{2\gamma}}$ | negative |
| 0                    | pushed   | $\frac{1}{\sqrt{2}}$                  | $O(\varepsilon^2)$           | $-\frac{3}{\sqrt{2}}$   | negative |
| $(0, \frac{1}{2})$   | bistable | $\frac{1}{\sqrt{2}} - \sqrt{2}\gamma$ | $O(\varepsilon^{1+2\gamma})$ | $\frac{\Gamma(4)}{\Gamma(1+2\gamma)\Gamma(3-2\gamma)} \frac{\sqrt{2}\gamma}{(1+2\gamma)^{2\gamma}}$ | positive |

in those regimes.

The transition between the various propagation regimes in dependence of  $\gamma$  is reflected in the leading-order asymptotics of  $\Delta c$ , as observed already in [15, 16] as well as in [4, 10, 17]. Thus, for instance, the power of  $\varepsilon$  in the expansion in (27) tends to zero as  $\gamma \rightarrow -\frac{1}{2}^+$ . Correspondingly, the leading-order coefficient  $K_\gamma$  is no longer given as in (27) in that limit, since one can show that the estimate for  $\widehat{Z}^-$  in (32) breaks down; the correct expression for  $K_{-\frac{1}{2}}$  can be found in (45). Similarly,  $K_\gamma$  vanishes as  $\gamma \rightarrow 0$ , where the limit can be taken either from the left or from the right. Hence, the leading term in the  $\varepsilon$ -asymptotics of  $\Delta c$  in (27) is of the order  $O(\varepsilon^2)$  in that case; see Table 5 for a summary of the asymptotic structure of  $\Delta c$  for  $\gamma \in [-1, \frac{1}{2})$ . In general, we remark that  $\Delta c$  becomes markedly more singular in the transition between the pushed and pulled regimes, as an expansion in (fractional) powers of  $\varepsilon$  is replaced by a logarithmic  $\varepsilon$ -dependence. Correspondingly, the correction  $\Delta c$  to the front propagation speed that is due to a cut-off is weaker in the bistable [15] and pushed propagation regimes [16] (sublinear or superlinear in the cut-off parameter  $\varepsilon$ , respectively) than it is in the pulled regime [6]. (This distinction is again obvious from the dynamics in the intermediate region: since the  $Z$ -direction is strongly repelling for  $P_-$  in the former two regimes, while it is merely weakly repelling in the latter,  $\Delta c$  has to be asymptotically weaker if a connection between  $P^-$  and  $P^+$  is to be achieved for  $\varepsilon \in (0, \varepsilon_0]$ .) Moreover, our analysis confirms that the correction  $\Delta c$  is negative for  $\gamma \in [-1, 0]$ , *i.e.*, when the reaction function  $f$  in (5) is of type I and the rest state at 0 is unstable, whereas it is positive when  $f$  is of type II or, equivalently, when  $\gamma \in (0, \frac{1}{2})$  and the zero state is (meta)stable, as observed previously [3]. In fact, the sign of  $\Delta c$  can be inferred directly from the dynamics in the intermediate region, as found already in [25]: since the  $W$ -coordinates of  $P_-$  and  $P_0^+$  are given by  $\lambda^\pm$  and  $-c_0$ , respectively, it follows from Table 5 in combination with Figure 3 that  $\Delta c$  is positive (negative) for  $\lambda^\pm < -c_0$  ( $\lambda^\pm \geq -c_0$ ). Finally, we remark that our predictions are supported by numerical simulations of the cut-off traveling front equation (6) (data not shown), which indicate, in particular, that satisfactory agreement between  $c$  and its first-order truncation in (36) can only be expected for very small values of  $\varepsilon$ ; see also [33], where bounds derived for  $c$ , in the context of the cut-off KPP equation, were shown to be valid merely up to  $\varepsilon = o(10^{-7})$ .

Next, we emphasize that the determination of the leading-order  $\varepsilon$ -asymptotics of  $\Delta c$  in the bistable and pushed propagation regimes requires explicit knowledge of the linear term (in  $\Delta c$ ) in the expansion for  $\mathcal{W}^u(Q_\varepsilon^-)$  defined in (10) [15, 16]. That term can be obtained from the solution of the variational equation (11), which is known explicitly for any  $\gamma \in [-\frac{1}{2}, \frac{1}{2})$  and which depends significantly on the value of  $\gamma$ : specifically,  $\frac{\partial v}{\partial c}(u, c_0)$  has a branch point at zero for  $\gamma \in (0, \frac{1}{2})$ , *i.e.*,  $\frac{\partial v}{\partial c} \rightarrow \infty$  as  $u \rightarrow 0^+$ , while the corresponding limit is well-defined for

$\gamma \in [-\frac{1}{2}, 0]$ ; cf. Equation (31). In particular, when  $\gamma = 0$ , we have  $\frac{\partial v}{\partial c} = -\frac{1}{3}(u - 1)$  and, hence,  $\lim_{u \rightarrow 0^+} \frac{\partial v}{\partial c} = \frac{1}{3}$  [20]. In the pulled regime, *i.e.*, for  $\gamma \in [-1, -\frac{1}{2}]$ , on the other hand, knowledge of the constant term (in  $\Delta c$ ) in (10) – or, rather, of the small- $u$  asymptotics of that term – is sufficient. Correspondingly, the leading-order coefficient in the asymptotics of  $\Delta c$  is universal, *i.e.*, cut-off independent, in the pulled propagation regime [6], whereas it depends substantially on the choice of  $\theta$  in the bistable [15] and pushed regimes [16], as suggested previously in [5] and in [10, 17], respectively.

Finally, our analysis shows that the cut-off Equation (5) supports a unique front solution, irrespective of the propagation regime under consideration. In particular, as the Heaviside cut-off  $H$  defined in (4) cancels the reaction terms in (5) in the inner region, the origin  $Q_\varepsilon^+$  is a saddle-node in the limit as  $\varepsilon \rightarrow 0^+$ , with a unique stable manifold that corresponds to the singular front in (7).

**Remark 13.** As an aside, we remark that the above classification allows for a geometric interpretation of the ‘critical’ front speed in Equation (7) (without cut-off) [7, 34], in the context of the equivalent first-order system (9): in the bistable regime, only orbits that lie on the (unique) stable manifold of the saddle equilibrium at  $Q_0^+$  can asymptote into  $Q_0^+$  as  $\xi \rightarrow \infty$ , *i.e.*, the critical speed is simply the propagation speed of the unique traveling front solution to (7). By contrast, any orbit of (9) is asymptotic to  $Q_0^+$  when that point is a node: in the pushed regime, orbits on the strong stable manifold of  $Q_0^+$  exhibit the strongest (exponential) decay in  $\xi$ ; the critical speed is defined as the speed of the corresponding front solution in that case. In the pulled regime, all (relevant) orbits decay at the same (algebra-exponential) rate, as  $Q_0^+$  is a degenerate node; correspondingly, the critical speed is given by the minimum speed for which (7) supports propagating fronts. An in-depth discussion of critical front speed phenomena can *e.g.* be found in [6, 7, 34].  $\square$

#### 4. Discussion

In this article, we have classified the effects of a Heaviside cut-off on the front propagation dynamics of the classical Nagumo equation [1, 2] in dependence of a control parameter. We have outlined a constructive, geometric proof for the existence and uniqueness of traveling fronts in the presence of a cut-off; moreover, we have deduced the leading-order asymptotics (in the cut-off parameter  $\varepsilon$ ) of the correction  $\Delta c$  to the front propagation speed  $c_0$  that is induced by the cut-off. Finally, we have determined explicitly the corresponding coefficients in the resulting expansions; our findings are summarized in Table 5. Our analysis is based on the geometric framework that was first proposed in [6], in the context of the cut-off Fisher-Kolmogorov-Petrovskii-Piscounov (FKPP) equation.

We remark that Equation (2), as well as its cut-off counterpart in (5), constitute ideal prototypes for a systematic geometric classification of front propagation in scalar reaction-diffusion equations of the type in (1) (with and without cut-off). First, they realize the three ‘canonical’ front propagation regimes (pulled, pushed, and bistable) observed in these equations, as well as the respective boundary cases, as the real parameter  $\gamma$  is varied in  $[-1, \frac{1}{2}]$ ; cf. Sections 3.1 through 3.4 above. Second, they are ‘minimal’ representatives of the family of equations in (1), in the sense that other members of that family, such as the Schlögl equation [10, 25] or the (real) Ginzburg-Landau equation [10, 17], are equivalent to Equation (2) under linear coordinate transformations; see [15, 16] for details.

To the best of our knowledge, our work [6, 15, 16, 20, 21] represents the first instance of a rigorous proof for the existence and uniqueness of front solutions in the cut-off Nagumo equation (5) or, more generally, in the family of equations in (3). The leading-order  $\varepsilon$ -asymptotics of  $\Delta c$ , on the other hand, was derived previously by Benguria, Depassier, and co-workers [3, 4] as well as by Méndez, Campos, and others [10], via an integral variational principle [3]. Analogous results in the framework of matched asymptotic expansions [30] were *e.g.* obtained by Brunet

and Derrida [5] and by Kessler *et al.*; see [17] and the references therein. Our analysis confirms their findings, and contextualizes them in terms of the dynamics of the cut-off first-order system (8) in the intermediate region, after blow-up; in particular, it explains the asymptotic structure of the correction  $\Delta c = c - c_0$ , identifying the source of the fractional or logarithmic powers of  $\varepsilon$  that can occur in the corresponding expansions; moreover, it gives a geometric interpretation for the sign of that correction, as obtained previously in [4, 5, 10]. Finally, we remark that our results concur with those of [17], where an analogous classification was given, based on classical ‘mode counting’ arguments: as emphasized there, the pushed propagation regime, which exhibits ‘nonlinear (type II) marginal stability’ (in their terminology), represents an intermediate case between the ‘metastable’ (bistable) and the ‘unstable’ (pulled) regimes, in that it is more singular than the former, but more regular than the latter.

Given the existence and uniqueness of front solutions in the cut-off Equation (3), a natural next step is the investigation of the stability of these fronts. The underlying theory centers on the Evans function, which has been widely applied in the study of front propagation in reaction-diffusion systems without cut-off [35]. More recently [36, 37], a generalized Evans function has been defined in situations where the front solution decays only algebraically at the zero rest state and the essential spectrum of the associated stability operator has a branch point at the origin. The corresponding analysis is based on geometric desingularization and can be expected to be valuable in the context of Equation (3), as well.

An alternative approach to our geometric methodology, which has been widely applied in the analysis of front propagation in the presence of a cut-off [4, 33], relies on the integral variational principle developed by Benguria and Depassier [3]; roughly speaking, the traveling front equation that is associated with (3) corresponds to the Euler-Lagrange equation in that approach, while the Lagrange multiplier is given by the front propagation speed  $c$ . A preliminary discussion of the relationship between the two approaches, in the context of results obtained by Benguria *et al.* [4] in the bistable and pushed regimes, can be found in [20]; nevertheless, a more complete understanding of that relationship is still lacking.

An important aspect of the front propagation dynamics of Equation (1) (with and without cut-off) concerns the process of front speed selection: the selection mechanism is termed either linear or nonlinear, depending on whether the front is pulled or pushed. While no general selection criteria seem to be known, preliminary results in this direction have *e.g.* been obtained in [38, 39]; however, no precise characterization of the underlying mechanisms has as yet been developed. The classification outlined in Section 3.5, which is based on geometric desingularization (blow-up), might provide a starting point for such a characterization.

A natural extension of the geometric framework developed here, in the context of the scalar Equation (1), is the analysis of multi-component systems in more than one spatial dimension. As is well-known, front interactions in such systems can lead to the emergence of novel patterns, in particular when stochastic fluctuations are accounted for. Thus, Kessler and Levine [40] reported diffusive instabilities in a coupled two-species model with cut-off, while Zemskov and Méndez [41] observed bifurcation patterns in piecewise linear activator-inhibitor systems. The resulting two-parameter singular perturbation problems are bound to yield interesting asymptotics and warrant further investigation.

Another topic of substantial recent interest is the relationship between the deterministic (cut-off) Equation (3) and the discrete (many-particle) systems that it approximates. Previous work [13] has shown that the approximation provided by (3) is in good (qualitative) agreement with the underlying discrete dynamics as long as the number of particles in the system is sufficiently large, which makes an efficient numerical implementation crucially important. Although several *ad hoc* simplifications have been proposed to reduce the required computational effort, no systematic analysis seems to be available to date.

Deterministic cut-offs have been successfully employed in a number of applications and, in

particular, in the life sciences; however, the front propagation dynamics of the resulting cut-off equations has not been considered systematically thus far. Thus, the mean-field description of the evolution of RNA virus populations proposed in [14] predicted a divergent mean fitness; after introduction of a cut-off, the front propagation speed was found to depend logarithmically on a threshold concentration below which autocatalytic viral growth ceases. Similarly, in certain models of Darwinian evolution [42], a standard continuum approximation gave rise to finite-time singularities in the propagation speed, while a cut-off reproduced that speed correctly. Finally, the review of pattern-generating mechanisms in [43] has shown that cut-offs in the growth term can generate complex branching patterns. Additionally, there exist numerous biological models in which the inclusion of a cut-off will lead to a more realistic description of the modeled phenomena; see *e.g.* [44, 45].

Undoubtedly, there exist a variety of asymptotic techniques that can be brought to bear on the front propagation dynamics of Equation (3); however, as has become evident through recent work in this area, geometric desingularization (blow-up) is particularly well-suited to a systematic analysis of the (more general) family of equations in (1) [6, 7, 15, 16, 20, 21, 34]. One advantage of the geometric approach lies in its highly visual and intuitive appeal, which contrasts with many of the classical techniques; moreover, it supplies the rigor that the latter sometimes lack. The method of matched asymptotics [30], for instance, generally only produces formal expansions for the correction  $\Delta c$  to the front propagation speed that is due to a cut-off, while our approach systematically uncovers the structure of these expansions, relating them to well-defined geometric objects. The integral variational principle [3], on the other hand, allows for considerable freedom in the choice of suitable trial functions, especially in the pulled propagation regime [33]; correspondingly, it often only yields bounds for  $\Delta c$ . Similarly, the expansions for  $\Delta c$  obtained in [4], in the pushed and bistable regimes, are formal. By contrast, the geometric counterparts found in [6] and in [15, 16], respectively, are rigorous and exact. Finally, these alternative approaches typically only give the leading-order asymptotics of  $\Delta c$ , whereas geometric desingularization can in principle be applied to evaluate that asymptotics to arbitrary order [20].

While the existence and uniqueness of front solutions in the presence of a cut-off and the asymptotics of the corresponding front propagation speed are naturally studied in the context of the traveling front equation (6), other questions, such as the convergence of general solutions to traveling fronts, the time asymptotics of the associated transients, the rate of convergence of the front propagation speed to its asymptotic value, as well as, to some extent, the stability properties of front solutions, require an understanding of the dynamics of the partial differential equation (3). Starting with [46], there have been numerous attempts at developing a geometric (invariant manifold) theory for the latter. Thus, preliminary results in the context of certain hyperbolic-parabolic systems of partial differential equations were obtained in [47], based on the concepts of similarity variables and weighted spaces. It remains to be seen if geometric desingularization can be combined with these or similar techniques to investigate the front propagation dynamics of cut-off reaction-diffusion equations of the type in (3).

## References

- [1] Gilding B H and Kersner R 2004 *Travelling waves in nonlinear diffusion-convection reaction* (Progress in Nonlinear Differential Equations and their Applications vol 60) (Basel: Birkhäuser Verlag)
- [2] Keener J and Sneyd J 1998 *Mathematical physiology* (Interdisciplinary Applied Mathematics vol 8) (New York: Springer-Verlag)
- [3] Benguria R D and Depassier M C 1996 *Phys. Rev. Lett.* **77** 1171
- [4] Benguria R D, Depassier M C and Haikala V 2007 *Phys. Rev. E* **76** 051101
- [5] Brunet E and Derrida B 1997 *Phys. Rev. E* **56** 2597
- [6] Dumortier F, Popović N and Kaper T J 2007 *Nonlinearity* **20** 855
- [7] Popović N and Kaper T J 2006 *J. Dynam. Differential Equations* **18** 103

- [8] Panja D 2004 *Phys. Rep.* **393** 87
- [9] van Saarloos W 2003 *Phys. Rep.* **386** 29
- [10] Méndez V, Campos D and Zemskov E P 2005 *Phys. Rev E* **72** 056113
- [11] Sherratt J A and Marchant B P 1996 *IMA J. Appl. Math.* **56** 289
- [12] Brunet E and Derrida B 2001 *J. Stat. Phys.* **103** 269
- [13] Brunet E, Derrida B, Mueller A H and Munier S 2006 *Phys. Rev. E* **73** 056126
- [14] Tsimring T L, Levine H and Kessler D A 1996 *Phys. Rev. Lett.* **76** 4440
- [15] Dumortier F, Popović N and Kaper T J 2010 *Phys. D* **239** 1984
- [16] Dumortier F, Popović N and Kaper T J 2010 Wave speeds for pushed fronts in reaction-diffusion equations with cut-offs *Preprint*
- [17] Kessler D A, Ner Z and Sander L M 1998 *Phys. Rev. E* **58** 107
- [18] Dumortier F 1993 *Bifurcations and periodic orbits of vector fields* (NATO ASI Series C vol 408) ed D Schlomiuk (Dordrecht: Kluwer Academic Publishing) 19
- [19] Krupa M and Szmolyan S 2001 *SIAM J. Math. Anal.* **33** 286
- [20] Popović N 2010 A geometric analysis of front propagation in a family of degenerate reaction-diffusion equations with cut-off *Preprint*
- [21] Popović N 2010 A geometric analysis of front propagation in an integrable Nagumo equation with a linear cut-off *Preprint*
- [22] Chen Z X and Guo B Y 1992 *IMA J. Appl. Math.* **48** 107
- [23] Armero J, Sancho J M, Casademunt J, Lacasta A M, Ramírez-Piscina L and Sagués F 1996 *Phys. Rev. Lett.* **76** 3045
- [24] Fenichel N 1979 *J. Differential Equations* **31** 53
- [25] Popović N 2007 *Fluids and waves* (Contemp. Math. vol 440) (Providence, RI: Amer. Math. Soc.) 187
- [26] *Handbook of mathematical functions with formulas, graphs, and mathematical tables* 1974 ed M A Abramowitz and L A Stegun (New York: Dover Publications, Inc.) 9th printing
- [27] Chow S N, Li C and Wang D 1994 *Normal forms and bifurcation of planar vector fields* (Cambridge: Cambridge University Press)
- [28] Corless R M, Gonnet G H, Hare D E G, Jeffrey D J and Knuth D E 1996 *Adv. Comput. Math.* **5** 329
- [29] Popović N 2005 *J. Phys.: Conf. Series* **22** 164
- [30] Lagerstrom P A 1988 *Matched asymptotic expansions. Ideas and techniques* (Applied Mathematical Sciences vol 76) (New York: Springer-Verlag)
- [31] Popović N and Szmolyan P 2004 *J. Differential Equations* **199** 290
- [32] Popović N and Szmolyan P 2004 *Nonlinear Anal.* **59** 531
- [33] Benguria R D, Depassier M C and Loss M 2008 *Eur. Phys. J. B* **61** 331
- [34] Dumortier F, Popović N and Kaper T J 2007 *J. Math. Anal. Appl.* **326** 1007
- [35] Sandstede B 2002 *Handbook of dynamical systems vol 2* (Amsterdam: North-Holland) 983
- [36] Popović N and Szmolyan P 2010 Evans functions and blow-up for degenerate shock waves *Preprint*
- [37] Sandstede B and Scheel A 2004 *Discrete Contin. Dyn. Syst.* **10** 941
- [38] Benguria R D and Depassier M C 1994 *Phys. Rev. Lett.* **73** 2272
- [39] Lucia M, Muratov C B, and Novaga M 2004 *Comm. Pure Appl. Math.* **57** 616
- [40] Kessler D A and Levine H 1998 *Nature* **394** 556
- [41] Zemskov E P and Méndez V 2005 *Eur. Phys. J. B* **48** 81
- [42] Cohen E and Kessler D A 2006 *J. Stat. Phys.* **122** 925
- [43] Golding I, Kozlovsky Y, Cohen I and Ben-Jacob E 1998 *Phys. A* **260** 510
- [44] Hallatschek O and Nelson D R 2008 *Theor. Pop. Biol.* **73** 158
- [45] Yin J and McCaskill J S 1992 *Biophys. J.* **61** 1540
- [46] Henry D 1981 *Geometric theory of semilinear parabolic equations* (Lecture Notes in Mathematics vol 840) (Berlin: Springer-Verlag)
- [47] van Baalen G, Popović N and Wayne C E 2008 *SIAM J. Math. Anal.* **39** 1951